Contents lists available at ScienceDirect

Engineering

journal homepage: www.elsevier.com/locate/eng

Research
Laser Micro/Nano-Manufacturing—Review

面向精准医疗的基于多光子聚合的微纳制造

胡家睿[a,b], 任安[a,b], 吕为康[a,b], Abdellah Aazmi[a,b], 秦昌玮[a,b], 梁心怡[a,b], 许晓斌[c], 俞梦飞[d], 李颀[e], 杨华勇[a,b,*], 马梁[a,b,*]

[a] State Key Laboratory of Fluid Power and Mechatronic Systems, Zhejiang University, Hangzhou 310058, China
[b] School of Mechanical Engineering, Zhejiang University, Hangzhou 310058, China
[c] School of Materials Science of Engineering, Tongji University, Shanghai, 201804, China
[d] The Affiliated Stomatologic Hospital, School of Medicine, Zhejiang University, Hangzhou 310003, China
[e] Department of Polymer Science and Engineering, Zhejiang University, Hangzhou 310058, China

ARTICLE INFO

Article history:
Received 31 January 2024
Revised 12 August 2024
Accepted 14 October 2024
Available online 24 November 2024

关键词
多光子聚合
微纳制造
生物制造
生物医学应用
药物递送

摘要

用于递送、诊断和治疗的微纳米尺度工具的设计与制造，是其在精准医疗领域实现多尺度集成的关键。传统三维打印方法受精度限制，难以满足这类工具的制备需求。基于多光子聚合（MPP）的微纳制造是一种非接触、高精度的成形技术，已被广泛应用于微纳米领域，是构建与微纳米尺度相关精准医疗工具的一项有前景的技术。本文首先概述了基于MPP技术的基本原理以及在精准医疗中所需材料的类型；随后总结并归纳了其在不同生物医学场景中的应用，包括递送系统、微组织建模、外科手术与诊断。最后，从材料设计、工艺优化以及实际应用三个维度，讨论了基于MPP的微纳制造在精准医疗中的挑战与未来发展方向，以期突破当前的技术瓶颈。

1. 引言

近年来，精准医疗的快速发展推动了生物医学工程领域向小尺度设备设计转变，在疾病诊断、外科手术、疾病建模以及靶向药物递送等[1–3]应用场景中，亟需微纳制造技术的支持。这一需求的增长也大大促进了三维（3D）打印技术在生物医学中的广泛应用。传统的3D打印主要用于宏观尺度制备，例如，通过选择性激光烧结打印具有良好生物相容性的骨支架材料[4–5]以及通过挤出打印构建角膜基质[6]。尽管传统3D打印已经取得了显著进展，但微纳制造在生物医学领域仍处于起步阶段[7]。其中，材料选择和结构成形是微纳制造的两大核心挑战[1,8]。传统的生物制造方式，如挤出打印[9]、喷墨打印[10]、光刻成型（SLA）和数字光处理（DLP）[11–15]，在亚微米尺度精度方面存在局限。光刻技术虽然可以实现较高分辨率，但难以制备复杂3D结构[16]。

多光子聚合（MPP）是一种基于光诱导聚合反应的激光微纳制造技术，能够在高精度条件下制备复杂结构，已在药物递送和再生医学等微纳生物医学应用中得到广泛研究[17–18]。本文对基于MPP的生物医学应用进行了系统综述，特别关注其在精准医疗中的应用，并给出一套材料选择与微结构设计的策略。我们希望本文能够为该领域的

* Corresponding authors.
E-mail addresses: yhy@zju.edu.cn (H. Yang), liangma@zju.edu.cn (L. Ma).

英文原文：Engineering 2025, 49(6): 35–60
引用本文：Jiarui Hu, An Ren, Weikang Lv, Abdellah Aazmi, Changwei Qin, Xinyi Liang, Xiaobin Xu, Mengfei Yu, Qi Li, Huayong Yang, Liang Ma. Multiphoton Polymerization-Based Micro/Nanomanufacturing Toward Precision Medicine. *Engineering*, https://doi.org/10.1016/j.eng.2024.10.016

发展带来启发并加速其在生物医学中的转化应用。本文结构如下：第2节介绍MPP的基本原理，包括多光子吸收（MPA）理论、MPP设备及工艺流程；第3节综述用于生物医学的材料体系，包括商用光刻胶以及由光引发剂（PI）和光聚合物构成的配方体系；第4节围绕不同生物医学应用场景展开讨论，并分析当前应用中的局限；第5节总结MPP在精准医疗中的挑战与前景。

2. 基本原理

光子吸收过程可以按照单个量子事件中被吸收光子的数量分为单光子吸收[图1（a-i）]和MPA [图1（a-ii）]。MPP或多光子光刻（MPL）通常涉及双光子吸收（TPA）、三光子吸收以及更高阶X光子吸收过程。TPA的概念最早由Göppert-Mayer于1931年提出[19–20]。该理

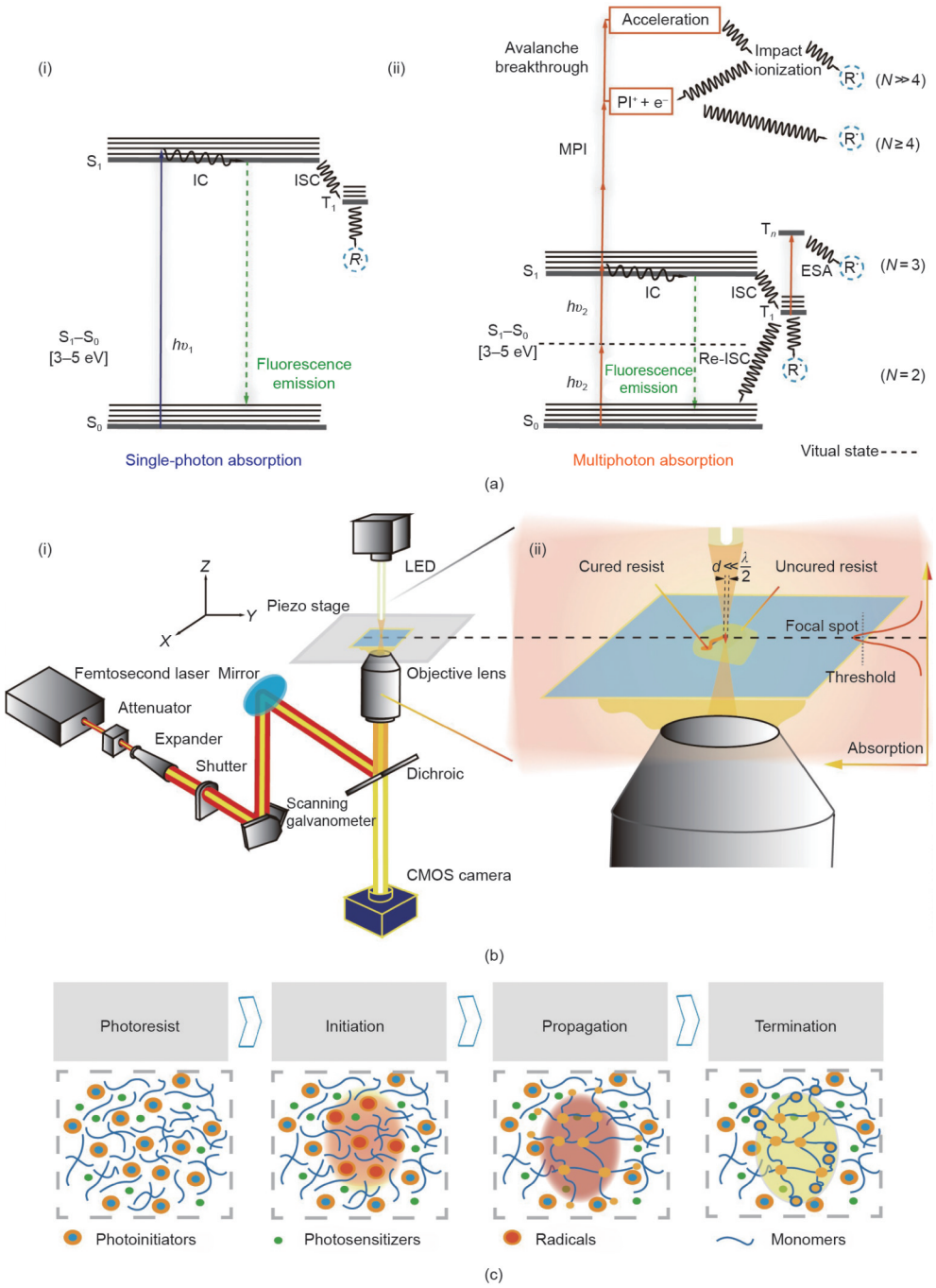

图1. 多光子聚合（MPP）的基本原理及基于MPP的微纳制造系统示意图。（a-i）单光子吸收过程；（a-ii）多光子吸收过程。S_0：基态；S_1：第一激发单重态；T_1/T_n：激发三重态；IC：内转换；MPI：多光子电离；ESA：激发态吸收；ISC：系间窜越。（b-i）基于MPP的微纳制造装置；（b-ii）焦点中心处光刻胶的聚合示意。LED：发光二极管；CMOS：互补金属氧化物半导体成像器件；d：MPP形成体素的横向尺寸；λ：飞秒激光波长。（c）光引发自由基聚合原理。图经参考文献[24]许可后转载。图中所有缩略语的定义都可在引用的参考文献中找到。

论描述如下：在一个量子事件中，两个光子与原子/分子发生相互作用，被分子选择性地“同时”吸收，从而为分子提供足够能量发生能级跃迁[图1（a-ii）]。直到1961年，Kaiser和Garrett [21]才首次在实验上观测到TPA现象。然而，TPA真正被引入制造领域已经是37年之后的1998年[22]，这一过程即所谓的双光子光刻（TPL）。这些吸收现象取决于光刻胶的吸收光谱与激发光波长之间的关系。第4节将进一步介绍MPL在微纳结构制备中的应用。

典型的MPL系统主要由飞秒激光光源及核心光路组成[图1（b）]，通常采用可调谐的超短脉冲飞秒激光，中心波长从可见光（VIS）到近红外（NIR）可选，具体取决于加工需求[23]。激光与物质的相互作用受多种因素影响，包括激光强度、曝光时间、光波长、偏振状态以及材料本身的性质等[24]。

如图1（b-i）所示，基于MPP的微纳制造设备一般工作过程为：飞秒激光先经准直后通过可调衰减器和扩束器，再通过快门，以控制曝光；随后通过*X*、*Y*扫描振镜，最终由二向色镜分光，根据不同波长分配光路。图1（b-ii）展示了通过物镜聚焦后，NIR或VIS光束在光刻胶的焦点区域诱导固化的过程。当焦点中心的激光功率强度超过阈值时，光刻胶中的单体在有或无PI存在的条件下均可发生聚合固化[25]，而未固化的光刻胶则在后续显影过程中被去除。整个打印过程通常在LED照明下，通过互补金属氧化物半导体（CMOS）相机进行实时观察。图1（c）展示了典型的MPL工艺，遵循光引发自由基聚合原理[26]。在自由基聚合中，光刻胶中的PI分子在特定波长与强度的光源（通常为NIR或VIS）照射下吸收两个及以上光子，被激发产生活性自由基或阳离子，进而在焦点平面中心区域引发单体或低聚物的聚合和交联，形成固体高分子网络[26]。这一过程持续进行，直到所有自由基通过偶合或歧化等途径相互反应而终止[27–28]。其聚合机理可以简化如下。

引发阶段：$\mathrm{I} \xrightarrow{x \cdot h\nu} \mathrm{R}^{\bullet}$

增长阶段：$\mathrm{R}^{\bullet} + \mathrm{M} \rightarrow \mathrm{RM}^{\bullet} \xrightarrow{\mathrm{M}} \mathrm{RMM}^{\bullet} \xrightarrow{\mathrm{M}} \mathrm{RM}_n^{\bullet}$

终止阶段：$\mathrm{RM}_n^{\bullet} + \mathrm{RM}_m^{\bullet} \rightarrow \mathrm{RM}_{n+m}\mathrm{R}$

式中，I为PI；M为单体；$\mathrm{R}^{\bullet}$为活性自由基；x为引发过程中吸收的光子数，且$x \geqslant 2$；$h\nu$为每个吸附光子的普朗克能量；n和m分别为增长和终止阶段聚合物中单体的数目。高效的PI与合适的光聚合物同等重要[28–29]。表1[30–34]总结了MPL中常用的飞秒激光光源及其关键参数。

表1 飞秒激光在MPL系统中的应用

Laser	Wavelength (nm)	Pulse properties	Numerical aperture (NA)	Refs.
Ti:Sa	810	80 MHZ, 100 fs	1.40	[30]
Ti:Sa	780	80 MHz, 100 fs	1.40	[31]
–	535	50 MHz, 270 fs	1.40	[32]
Ti:Sa	532	80 MHz, 100 fs	1.45	[31–32]
–	514	0.6 MHz, < 250 fs	1.40	[33–34]
Diode	405	1 MHz, 50–100 ns	1.40	[31,34]

3. 材料

用于MPL的材料大致可按功能分为三类：首先是单体/低聚物混合物，其作为结构基体，用于形成3D实体结构；其次是PI，其能够同时吸收多光子，产生活性中心并诱导聚合，可通过自身或与其他组分反应引发聚合[24,35–36]，有时还会加入交联剂和稳定剂——交联剂可提高打印分辨率和材料刚度[37]，稳定剂用于提高配方稳定性[38]，溶剂的选择取决于其他组分；再次是光敏剂（PS），其加速光引发过程，但自身通常不直接参与光聚合，须与PI组合使用。此外，通过在树脂中加入淬灭剂可以进一步提升3D打印的特征尺寸与分辨率[39]。

一般来说，MPL用材料应满足：

（1）对特定波长的入射光具有良好的透明性；

（2）为确保MPA并引发聚合，局部光强须高于PI的烧蚀/聚合阈值[40]，如图1（b-ii）所示。

用于生物医学应用时，MPL材料还须具备一定的打印窗口，以保证稳定可打印性。未来更加偏好天然来源材料。同时，材料应根据精准医疗应用需求，具备刺激响应性、高电导性、可调机械性能等功能[41–42]。

3.1. 商用光刻胶

3.1.1. IP系列光刻胶

IP系列光刻胶（Nanoscribe, Germany）是常用的负性光刻胶[43]，兼具良好的机械性能和生物相容性，因此在生物医学领域被广泛用于结构材料[44]。不同种类的IP光刻胶具有不同的打印特性，可覆盖多类应用场景：IP-L是一种丙烯酸类负性光刻胶[45]，收缩率低，特征尺寸在微米级，适合用于仿生表面等；IP-聚二甲基硅氧烷（PDMS）是一种弹性体，适于打印柔软、可大变形结构，如微流控和微机电系统（MEMS）结构[46]；IP-Q适合快速制备毫米级器件；IP-S为丙烯酸基负性树脂，表面平滑，用于制备微/中尺度细胞支架，具有光学级表面粗糙度和形状精度；IP-Dip是一种丙烯酸基光刻胶，可打印具有亚

微米特征和高纵横比的结构；IP-G用于油浸模式，便于获得亚微米特征且收缩率低；IP-Visio面向生命科学，适合高分辨率制造小尺度多细胞支架。

总而言之，IP系列光刻胶还常与其他功能材料组合以实现更多生物医学功能。例如，Serien和Takeuchi [47]将蛋白网络嵌入具有高机械强度的IP-L骨架，用于构建3D空间可编程蛋白刺激平台，以模拟3D微环境并研究细胞行为。综上，IP系列光刻胶因其机械性能可控、配方成熟而得到广泛应用。

3.1.2. ORMOCER® 光刻胶

ORMOCER® 光刻胶（Fraunhofer ISC, Germany）是一类有机-无机杂化材料，具有无机的–Si–O–Si骨架，并在侧链上带有可聚合的有机基团（如丙烯酸或环氧基）。这些有机侧链在紫外（UV）/VIS光照后可发生聚合，使材料同时具备有机材料与无机材料的优势：附着力好、机械/热稳定性高[48]。通过与生物基、可降解组分结合，可得到BioORMOCER®，推动可持续、生物可降解材料的发展[49]。ORMOCER®在400~1600 nm范围内具有良好光学透明性，并在NIR区域具有较低光损耗，是TPL的理想候选材料。凭借稳定的无机网络和低收缩（约2%），该光刻胶已被广泛用于药物递送微针及耳[50]和视网膜[51]植入物。

与SU-8（IBM, USA）或IP光刻胶相比，ORMOCER®更适用于组织工程领域，因为其机械/热稳定性更优。另外，BioORMOCER®具备较好的生物降解性，是极具潜力的光刻材料。

3.1.3. SZ2080™光刻胶

SZ2080™（IESL-FORTH, Greece）是一种应用广泛、具有良好生物相容性且可商业获取的杂化光刻胶。由于具备低收缩率、良好的力学性能和生物相容性，它被广泛用于细胞工程。例如，Malinauskas等[52]将SZ2080™用作细胞支架材料，并确定了包括平均激光功率、样品扫描速度和显影条件在内的最优微加工参数。在此前工作的基础上，Maciulaitis等[53]首次采用超快脉冲直写光刻技术，以SZ2080™作为支架材料制备具有3D微结构的支架，并在兔体内测试了其生物相容性。该研究的成功结果支持了如下假设：具有六边形孔结构的有机-无机杂化（HOI）微结构支架与软骨细胞接种相结合，可成功应用于软骨组织工程。Maciulaitis等[54]则研究了细胞支架的几何特征（如孔洞的形状和尺寸）对细胞增殖及软骨修复效果的影响。这些体外实验证明，与六边形孔支架相比，具有四边形孔结构的支架表现出更优的结果。他们的发现进一步引出了关于人源细胞HOI支架接种用于软骨修复的新假设。

尽管SZ2080™已被广泛用于细胞支架的制备，但其较差的生物可降解性在长期体内应用中仍然是一个重要挑战[53,55]。

3.1.4. SU-8光刻胶

SU-8是一种常用的环氧基负性光刻胶，因具有高热稳定性而在微流控、细胞支架等生命科学领域被广泛用作结构材料[56–57]，也是最常用的MPP负性光刻胶材料之一[58]。

通过引入功能材料，还可让SU-8适应更多生物医学场景。例如，Tottori等[59]利用SU-8经物理气相沉积Ni/Ti薄层制备磁性螺旋微机器，通过TPL实现3D成形，用于局部药物递送；Kim等[60]使用类似的方法制备微腔，用于3D细胞培养与靶向运输；Suter等[61]利用含11 nm磁铁矿纳米粒子（即Fe_3O_4）与SU-8的磁性聚合物复合材料制备游动微机器人，用于单细胞操控和药物递送；Peters等[62]基于Fe_3O_4纳米粒子/SU-8制备扭转型驱动器，实现复杂磁致驱动。

总的来看，SU-8具备高热稳定性、优良机械性能（杨氏模量约2~3 GPa）以及高屈服强度，非常适合作为高纵横比结构的基体。对于生物医学应用，需要进行表面改性和功能化来增强其与细胞、蛋白及其他生物组分的黏附性。

3.2. 非商用光刻胶

3.2.1. PI

PI在从微观反应到宏观结构形成的全过程中均起关键作用。对于双光子引发剂，其分子须同时吸收两个光子（每个光子能量相当于带隙的一半）才能跃迁至高能激发态并生成活性中心，进而触发后续聚合[63]。通过多光子引发形成的材料通常具有3D网络结构，并在整体机械性能（如黏度、强度）上得到增强。为了增强机械性能，PI在聚合中的作用更加重要。

要提升材料的可打印性，PI必须具有高灵敏度、高引发效率，可通过双光子吸收截面δTPA（Goeppert-Mayer, GM）衡量。δTPA越大，越适合作为TPA引发剂。Cumpston等[64]研究了PI的分子结构对δTPA的影响，总结出几种常见分子设计策略：①延长共轭π键体系；②采用稠合芳环π–π桥提高分子平面性；③引入强给电子/吸电子基团以增强分子内电荷转移；④引入具有高引发效率的功能基团。

在TPL过程中，生成的聚合物结构也会受到自由基以及其他活性基团的影响[64]。PI的选择通常基于材料的加工窗口，即在“扫描速度-激光功率”二维（2D）空间的可加工范围。加工窗口越大，说明PI越高效。除效率外，PI的生物相容性、水溶性和细胞毒性也是生物医学应用中不可忽视的参数。常见策略包括向疏水性PI中添加非离子表面活性剂（如Pluronic F127）以抑制聚集，增强水溶性[65–66]。

但过量的非离子表面活性剂会增加PI的细胞毒性。为兼顾水溶性与生物相容性，研究者尝试将油溶性PI包封于环糊精或葫芦脲等超分子疏水腔体中，通过主客体作用提高其水溶性和生物相容性[67–71]。

尽管已有部分工作[25,72–75]探索了无PI的MPL路线，但在大多数光刻胶配方中，PI仍是不可或缺的一环。因此，在效率与生物安全之间取得平衡仍是MPL生物医学应用中PI设计的核心问题。表2 [63,70,76–96]列出了生物医学中常用的一些PI及其参数。

3.2.2. 光聚合物

光聚合物大致可分为有机、无机、天然与合成四大类。本文重点讨论与生物医学相关的天然来源光聚合物与合成光聚合物，以便更好理解其生物相容性与功能性。天然光聚合物（如胶原和明胶）是细胞外基质（ECM）的重要组成部分，显著影响细胞微环境的机械性质[7,18]；合成光聚合物[如聚乙二醇（PEG）]则是常见功能材料的基础[97]。此外，我们单独讨论在未来极具潜力的智能/响应性材料。

（1）天然来源光聚合物。胶原基材料：胶原是哺乳动物ECM中最主要的结构蛋白，占体重约30% [98]，广泛分布于皮肤、骨骼等组织，在多种细胞的生理和生化行为中起关键作用，因此在过去几十年中备受关注[99]。然而，胶原的批次间差异较大，其机械和生物学性质会受到生产条件（如温度）的影响[100]。此外，天然胶原不易直接参与光交联，往往需要额外引入可光聚合基团或与其他材料共混。

对于组织工程而言，理想的生物材料需要良好的可重复性与高制造精度。Tytgat等[101]将I型重组胶原（RCPhC1）分别功能化为甲基丙烯酰胺（RCPhC1-MA）、降冰片烯（RCPhC1-NB）和巯基（RCPhC1-SH）衍生物，使其可在TPL下实现高分辨率3D打印。但胶原基光聚合物仍存在一些局限性。胶原蛋白来源复杂导致其性质差别较大，因此在不同生物医学领域应用时必须对胶原蛋白的来源和提取方法进行深入研究。另外，胶原蛋白的机械性能较弱，尤其在干燥状态下十分脆弱，使显影等过程窗口狭窄，限制了其应用范围。

明胶基材料：明胶由I型胶原部分降解获得，保留了精氨酸-甘氨酸-天冬氨酸（Arg-Gly-Asp）序列，可促进细胞黏附和增殖[102–103]，同时具有良好的生物降解性，在生物医学领域应用广泛[104–106]。但其本身机械性能欠佳，体内生物相容性和稳定性仍需改善。明胶的上临界溶解温度低于体温[107–108]。

2000年，Van den Bulcke等[109]通过引入甲基丙烯酰胺（MA）基团合成了明胶甲基丙烯酰胺（GelMA）水凝胶，此后GelMA由于可调物理属性与优异生物相容性在生物医学中被广泛使用。良好的生物相容性使明胶衍生物（包括基于GelMA的水凝胶）成为TPL中另一类主要的光交联生物材料。GelMA的优势在于：其机械性能可以通过多种方式调节[110–111]，如改变PI类型、光交联时间、浓度[112]等，从而满足不同场景下的需求。Schuurman等[113]报道称，光交联持续时间与弹性模量呈正相关。GelMA基水凝胶已被广泛用于药物递送等领域[114]，具备良好的孔隙结构、可降解性和膨胀/力学可调性。

但GelMA也存在抗压强度低（2~30 kPa）、体内降解较快（7 d、28 d分别降解32%、52%）等问题，限制了其在长期体内应用中的表现[99,115]。

牛血清白蛋白（BSA）基材料：BSA是MPL中常用的蛋白质之一，具有显著的刺激响应特性。Kaehr和Shear [116]提出利用MPL制备具有良好刺激响应性能的亚微米BSA结构。Chan等[117]利用BSA制备具有亚微米拓扑特征的复杂微结构，并通过研究其降解性、细胞相容性和细胞-基质相互作用，展示了其在生物医学中的应用潜力。

但蛋白质基光聚合物整体上机械稳定性较差，通常需要与其他聚合物形成杂化网络以增强机械强度。Engelhardt等[85]制备了聚合物-蛋白质杂化结构。许多蛋白（包括BSA）在脱水后容易变脆[118]，需要在应用前改善其机械性能。由于BSA对光、热和pH极为敏感，其结构稳定性也较差，并不适合对结构长期稳定要求较高的医疗场景。

透明质酸（HA）基材料：HA是人体ECM的重要成分之一，因而是构建组织工程支架的理想候选材料。但类似其他天然材料，HA的机械性能较弱，须通过化学修饰增强，以适应TPL；同时要确保足够的生物相容性。Kufelt等[119]将HA与聚（乙二醇）二丙烯酸酯（PEGDA）结合，制备共聚物，并引入人表皮生长因子以提高生物活性。在TPL制备的支架上进行细胞增殖实验，证明其具有良好生物相容性。

近年来出现了多种HA改性策略，如HA乙烯基酯

表2　生物医学应用中常用的PI

Watersolublility	Solubility ($mg \cdot mL^{-1}$)	PI	δTPA (wavelength) (solvent)	Molar extinction coefficient ε_{max} at λ_{max} (solvent)	Single-photon absorption maximum λ_{max} (solvent)	Monomer and application	Refs.
Insoluble in water	0	Irgacure 369	7GM (—) (—)	—	324nm (—)	PEGDA, 3D scaffolds for optical interrogation; neurite guidance of human iPSC-derived neuronal networks	[63,76]
	—	Bis(styryl)benzene-derivatives	1940 GM (835 nm) (—)	—	472 nm (—)	— Guidelines for bioimaging applications	[77,78]
	—	Coumarin derivatives (e.g.,DEDC)	29.5 GM (800 nm) (chloroform)	5.23×10^4 $mol^{-1} \cdot L \cdot cm^{-1}$ (chloroform)	438 nm (chloroform)	— Two-photon excited-photodynamic therapy (PDT)	[79,80]
	—	Triphenylamine derivatives bearing formyl groups	—	—	375 nm (dichloromethane)	MAPTMS, ZPO, and DMAEMA or MAA, microscaffold in biomedical applications	[81]
Water-soluble	5	Irgacure 2959	—	2.96×10^2 $mol^{-1} \cdot L \cdot cm^{-1}$ (methanol)	328 nm (methanol)	Methacrylate chitosan, 3D ring-like microscaffolds for human pulmonary microvascular endothelial cells culture	[82–84]
	100	RB	10 GM (800nm) (water)	—	548 nm (acetate)	Gelatin methacrylamide and BSA, 3D polymer-protein hybrid scaffolds	[85,86]
	40	MB	—	8.5×10^4 $mol^{-1} \cdot L \cdot cm^{-1}$ (water)	664 nm (water)	BSA, potential for regenerative medicine	[87,88]
	High	carboxylate sodium salts of cyclic benzylidene ketone, e.g., P2CK	176 GM (800nm) (water)	5.50×10^4 $mol^{-1} \cdot L \cdot cm^{-1}$ (water)	506 nm (water)	PEGDA, tissue engineering	[89–92]
	—	Carboxylate sodium salts of cyclic benzylidene ketone, (e.g., G2CK)	163 GM (800 nm) (water)	—		gelMOD, cellular microarrays to study cell behavior	[92]
	400	Xanthene dyes (e.g., Eosin Y)	10GM (800 nm) (water)	—	524 nm (water)	—, two-photon excited-PDT	[86,93]
	29	LAP	—	—	375 nm (water)	PEGDA, functional structures to study cell behavior	[94]
	120	WSPI	360 GM (730 nm) (water)	4.9×10^4 $mol^{-1} \cdot L \cdot cm^{-1}$ (water)	423 nm (water)	PEGDA, 3D woodpile scaffolds in living organisms	[95,96]
	—	BMVPC/CB7	2999 GM (—) (water)	—	471 nm (water)	PEGDA, 3D woodpile scaffolds for tissue engineering	[70]

BSA: bovine serum albmin; BMVPC: 3,6-bis[2-(1-methyl-pyridinium)vinyl]-9-pentyl-carbazole diiodide; CB7: cucurbit[7]uril; DEDC: 7-diethylamino-3-2'-benzimidazolyl) coumarin; DMAEMA: 2-(dimethylamino) ethyl methacrylate; Eosin Y: 2-(2,4,5,7-tetrabromo-6-oxido-3-oxo-3*H*-xanthen-9-yl) benzoate; G2CK: 4-methylcyclohexanone; gelMOD: methacrylamide-modified gelatin; Irgacure 2959: 2-hydroxy-4'-(2-hydroxyethoxy)-2-methyl-propiophenone; Irgacure 369: 2-benzyl-2-(dimethylamino)-1-[4-(morpholinyl) phenyl)]-1-butanone; RB: rose bengal; MB: methylene blue; LAP: lithium phenyl(2,4,6- trimethyl benzoyl) phosphinate; MAA: methacrylic acid; MAPTMS: methacryloxypropyl trimethoxysilane; PEGDA: poly(ethylene glycol)diacrylate; P2CK: 3,3′(((1E, 1′E)-(2-oxcyclopentane-1,3-diylidene)bis(methanylylidene))bis (4,1-phenylene)bis(methylazanediyl))dipropanoate; WSPI: 1,4-bis(4-(*N*, *N*-bis(6-(*N*,*N*,*N*-trimethylammonium)hexyl)amino)-styryl)-2,5-dimethoxybenzene tetraiodide; ZPO: zirconium *n*-propoxide.

（HAVE）[120–122]和HA甲基丙烯酰胺（HAMA）[123]。Duan等[124]对HAVE前驱体的TPL光刻胶进行了性能研究，显示其在制造高精度细胞支架方面具有潜力。因此，基于HA的材料可被视为未来精准医疗应用的潜在材料。

与其他天然材料类似，基于HA的光聚合物具有一般的机械性能，如低抗压强度（1~10.6 kPa）。不过，HAMA在磷酸盐缓冲盐水（PBS）中降解率高，第20天可达80% [115]。这些发现为HA材料的功能化提供了广泛的研究方向。

（2）合成材料。PEG基材料：PEG基水凝胶是细胞与组织工程中使用最广泛的构筑材料之一。PEG具有拒蛋白和抗血小板黏附的特性，可在一定条件下减少血栓形成[125–130]；同时具备优良的亲水性及在多种有机溶剂中的溶解性[131–132]。PEG常被用于提升生物药物稳定性和在体内的停留时间，并用于抑制非特异性蛋白吸附[133–134]，因此PEG基药物载体在近年的药物递送中被广泛关注。

然而PEG是一种不可生物降解的聚醚，通常被认为免疫原性与抗原性较低，但其在一些慢性体内应用中表现不佳[135–136]。PEG还缺乏细胞黏附位点，限制了其在体内的长期生物医学应用[115]。因此，PEG常与其他材料共混或进行进一步修饰。

聚酯（PE）基材料：PE基材料因其机械性能可调，在生物医学领域应用广泛[137]。Melissinaki等[138]利用TPL制备聚交酯（PLA）基3D神经组织工程支架，通过引入甲基丙烯酰基团，使PLA可在NIR照射下固化；PLA共聚物系统也可通过调整组成获得不同物理性能。聚己内酯（PCL）系材料则常用于高分辨率结构打印。Thompson等[139]研究了不同PCL基材料在TPL条件下的最小激光功率与分辨率，用于视网膜细胞替代治疗模型。通过增加聚（ε-己内酯）二丙烯酸酯（PCLDA）和聚（ε-己内酯）三丙烯酸酯（PCLTA）的分子量，聚合所需的激光功率略有增加。此外，无论其分子量如何，在所有扫描速度下，PCLDA聚合所需的激光强度远高于PCLTA。基于PCLTA的结构的保真度也可以通过不同的聚合物浓度进行调谐，为视网膜细胞接种的高分辨率模型制备开辟了新途径。

综上所述，PE基材料凭借其可调的机械性能和成本优势被视为组织工程及其他应用领域的理想候选材料。

PDMS基材料：PDMS由于透明和弹性，在微流控领域应用极为广泛[140–146]。为了拓宽MPL材料的范围，许多研究者研究了基于PDMS材料的机理和性能。Coenjarts和Ober [147]首次利用双光子3D微制造制备PDMS微结构，通过光氢硅化反应和自由基交联反应两种途径获得单体素纵横比为3~4的结构，显示了其在复杂微流控系统中的潜力。Hasegawa等[148]开发了可光固化PDMS树脂用于TPL制造3D微机器；展示了在微流控器件中的应用潜力以及作为生物应用微操作工具的潜力。Rekštytė等[149]研究了掺杂不同PI的PDMS在不同曝光条件下的3D成形，获得约5 μm的分辨率与720 $\mu m^3 \cdot s^{-1}$的成形速率，展示了其在生物医学支架中的应用前景。

不过，PDMS自身含有大量–CH_3基团，表面高度疏水[150–152]，在接触液体生物样品时可能产生限制[153]，常需表面等离子体处理或涂层改性。

其他合成体系：除了上述光聚合物之外，其他材料也具有出色的机械性能。例如，Buchroithner等[154]提出了两种新型生物相容树脂BisSR和M10，用于体内组织工程。M10的杨氏模量随激光强度变化在40~120 MPa之间，BisSR则约为80 MPa且与写入参数无关。Men等[155]提出了一类具有可调机械性能（杨氏模量：0.3~1.43 GPa）且具良好生物相容性的TPL可打印聚合物，适合用于生物器件。总之，MPL可用于制造具有优异机械性能的材料和光聚合物，用于组织工程等应用领域。

（3）智能材料。所谓智能材料/主动材料，是指能随时间或在环境刺激发生形状或尺寸变化的材料。常见制备方法[156–157]包括在光聚合物中掺杂功能纳米颗粒或进行表面沉积等。Xia等[158]将带有甲基丙烯酰基的Fe_3O_4纳米颗粒掺入光刻胶中，通过MPL制备远程磁控制微机器；Tottori等[159]在螺旋微机器表面沉积Ni/Ti双金属薄层，实现磁驱动并改善表面生物相容性。

利用光聚合网络本身的特性也可获得智能响应结构，如基于BSA的光/热/pH响应水凝胶[159–161]。液晶弹性体（LCE）[156]、响应性水凝胶[162]与形状记忆聚合物（SMP）[157]均是典型代表。Martella等[163]制备了光响应液晶网络并通过MPL制备微执行器，可通过调节交联剂含量控制其从微观到宏观的变形动力学；Zeng等[164]制备具有完全可逆光响应机械行为的LCE结构，能够在光照下产生约20%的可逆收缩；Martella等[165]制作了可通过光照控制的“微型手”，用于抓取并区分不同颜色/灰度的微粒；除了LCE，SMP也是生物医学应用中MPL的候选材料。Elliott等[166]合成并用TPL制造了苄基甲基丙烯酸酯基SMP 3D结构，可在温度变化条件下实现任意3D形状的形变，具有应用于视网膜血管支架等微型可展开医疗器械的潜力。表3 [123–124,139,147–149,167–182]对MPL中常见的光聚合物进行了汇总。

总的来说，为多光子3D激光打印开发新型功能性和主动材料，已在近年呈快速增长趋势，并推动了包括生物医学在内的诸多应用场景。

表3 生物医学应用中的光聚合物

Type	Source	Example	Characteristics	Degradation	PIs	Applications	Refs.
Synthetic	PEG-based	PEGDA/PETA	Antiswelling and high strength	Nonbiodegradable	Irgacure PI	Drug delivery	[167]
		PEGDA	Antiswelling and high strength	Nonbiodegradable	Riboflavin-TEOHA mixture	Engineering scaffolds	[168]
		PEGDMA	Antiswelling and high strength	Nonbiodegradable	Irgacure 369	Drug delivery	[169]
		PEGA	Antiswelling and high strength	Nonbiodegradable	TEA	Drug delivery	[170]
	PE-based	Acrylate-end-capped urethane-based PCL	Tunable mechanical properties	Nonbiodegradable	Irgacure 2959	Cell scaffolds	[171]
		PLA-PCL	Tunable mechanical properties	Nonbiodegradable	Irgacure 369/BA740	Cell scaffolds	[172]
		PCLTA/PCLDA	Tunable mechanical properties	Nonbiodegradable	Irgacure 369	Retina cell delivery scaffolds	[139]
	PDMS-based	PDMS-based liquid	Elastomeric properties	Nonbiodegradable	Isopropyl-thioxanthone	Potential for microfluidic systems	[147]
		A photocurable PDMS resin	Elastomeric properties	Nonbiodegradable	Unknown	Microdevices in microfluidic systems	[148]
		Commercial PDMS kit	Elastomeric properties	Nonbiodegradable	THIO; ISO; and IRG2	Microstructure in microfluidic systems	[149]
	Others	AAm/AA/MBAAm	Photoresponsive	Nonbiodegradable	Bis(styryl)benzenederivatives	Microfluidic systems	[173]
		NIPAAm	Temperature and pH stimulus	Nonbiodegradable	LAP	Drug delivery	[174]
		PETA/PNIPAAm/ PNIPAAm-AAc	—	Nonbiodegradable	LAP; TEA (Ecos-1)	Helical microrobot, photothermal treatment of cancer cells	[175]
		HeMA/MMA	—	Nonbiodegradable	—	Drug delivery	[176]
		MMA	—	Nonbiodegradable	Ivocerin	Drug delivery	[176,177]
Natural-derived	Protein-based	GelMA	Biocompatible	Biodegradable	Irgacure 2959	Tissue engineering	[178]
		BSA	pH-stimulus	Biodegradable	RB	Microrobots *in vivo* biomedical task and proto-tissue engineering	[179]
		Collagen	Biocompatible	Biodegradable	Riboflavin	*Ex vivo* human corneal lenticule	[180]
		Concanavalin A	Biocompatible	Biodegradable	RB	Modal scaffold and extracellular matrices	[181]
		Fibronectin	Biocompatible	Biodegradable	RB	Modal scaffold and extracellular matrices	[181]
		Fibrinogen	Biocompatible	Biodegradable	RB	Modal scaffold and extracellular matrices	[181]
		SF	Biocompatible	Biodegradable	Ru/SPS	Potential for tissue engineering	[182]
	HA-based	HAMA	Biocompatible	Biodegradable	HMPP	Stimulus-response structure for biomimetic field	[123]
		HAVE	Biocompatible	Biodegradable	P2CK	Cell scaffolds	[124]
	Others	Chitosan (assist)	Biocompatible	Biodegradable	PS: Irgacure 369; PI: benzil	Potential for scaffold in tissue engineering	[178]

AA: acryolylacetone; AAc: acrylic acid; AAm: acrylamide; HeMA: hydroxyethyl methacrylate; IRG2: 2-benzyl-2-(dimethylamino)-4'-morpholinobutyrophenone; ISO: isopropyl-9H-thioxanthen-9-one; Ivocerin: bis-4-(methoxy benzoyl)diethyl germanium; MMA: methyl methacrylate; NIPAAm: *N*-isopropyl acrylamide; MBAAm: *N*,*N*'-methylene bisacrylamide; TEA: *N*,*N*,*N*-triethanolamine; THIO: thioxanthen-9-one; PE: polyesters; PEGDMA: poly(ethylene glycol)dimethacrylate; PEGA: poly(ethylene glycol)acrylate; PEGDA: poly(ethylene glycol)diacrylate; PETA: pentaerythritol triacrylate; SF: silk fibroin; HMPP: 2-hydroxy-2-methylpropiophenone; PNIPAAm: Poly(*N*-isopropylacrylamide); SPS: 3,3'-dithiobis-1-propanesulfonic acid; TEOHA: triethanolamine.

4. 生物医学应用

医疗器械的微型化为病人诊断和治疗提供了更先进的解决方案[183]。同时，精准医疗对个体诊断和治疗的精度要求极高，这也使得各类生物医学应用中小尺度制造需求愈发突出。MPL能够制备可用于诊疗的微纳器件。根据精准医疗不同场景，本文将这些器件归纳为四类：递送系统、微组织建模、手术、诊断。

4.1. 递送系统

MPL可用于制备精确药物递送与物质释放系统，这是精准医疗中的核心环节。根据递送对象不同，递送装置可大致分为两类：微机器人和微针。微机器人主要用于体内靶向应用，而微针主要用于体外透皮和局部组织的递送。

4.1.1. 药物递送

（1）微机器人：MPL能够制备复杂的微纳结构，因此广泛用于制备具有可控轨迹与可编程释药行为的微机器人。精确的轨迹控制直接关系到药物的靶向能力，而轨迹控制受驱动方式和结构设计共同影响。最主流的驱动方式是磁驱动，它具有非接触、对生物组织无电磁干扰、轨迹高度可控等优点[184–186]，可将载药载体导航至体内特定病灶[187–188]。除此之外，还有光[189]、热[190]、化学反应[191]以及声学[192]等驱动方式。

研究人员已致力于提升体内给药治疗中轨迹控制的精准度[193]。Ceylan等[114]制备了一种可降解双螺旋微游泳器，在旋转磁场作用下可携带一定负载并实现可控游动，并在金属蛋白酶作用下降解为无毒产物[图2（a）]；Xin等[194]设计了锥形中空微螺旋结构，相较直螺旋具有更强游动能力与更小横向漂移；Xu等[195]提出“精子-微马达”混合系统[图2（b）]，将化疗药物装载于精子中，并设计一个可在撞击肿瘤后释放精子的微马达夹具，通过精子-肿瘤细胞膜融合实现药物释放，为女性生殖系统疾病提供一种生物兼容的靶向递送平台。

药物释放方面，研究主要集中在控制释放时间、剂量与频率。药物释放方法根据应用需求来确定，为此设计了不同的刺激响应材料和结构以实现药物释放。刺激响应性包括材料对体内pH、温度及其他传统物理量变化的反应，以及对特定物质（如酶）的反应[114]。

释放策略既依赖结构设计（多阶段释放腔体、低阻力通道等），也依赖材料特性（如生物相容性以及pH、温度、光响应等）。Lee等[175]仿生花粉外形，利用具有温度响应的表面能调控结构，并通过磁驱动与pH响应控制药物释放；Song等[196]利用马勃菌（puffball）结构设计高装载量、多级释放的微机器人[图2（c）]，通过NIR光热封层实现可控释药周期；此外，NIR密封层促进了受控药物释放，并实现了精确且可控的药物释放时间。除了药物释放时间和剂量外，多重药物释放对精准药物递送系统来说也至关重要。基于多药物释放结构，Li等[197]设计了“仿鱼”异质微机器人，该机器人可同时携带阿司匹林和多柔比星（DOX）实现协同抗癌治疗。

在材料层面，研究主要聚焦基于刺激-响应材料的药物释放。简单来说，刺激主要分为内源性刺激（如pH、温度、氧化还原、酶）与外源性刺激（如光、电、磁）[198]。载药的装置可以根据正常生理环境与体内肿瘤区域特性的差异自动响应刺激。因此，内部刺激被视为至关重要。肿瘤区域内pH的变化是载药结构设计的基础。Ye等[199]将叶酸（FA）/GelMA与磁性金属有机框架（MOF）结合，制备了可在弱酸环境中降解并释放药物的微机器人。含FA的微机器人对癌细胞抑制率高达93%，而不含FA的对照组中这一比率仅为78%。Xin等[200]设计了pH响应-磁驱动的“变形鱼”（SMMF），通过“嘴”部开闭实现DOX的pH触发释放[图2（d）]，且其对PH的响应范围从NaOH溶液中的9降至PBS中的7.4，更接近生理条件。基于他们之前的研究结果，Xin等[201]进一步改进了印刷工艺，克服了单一材料印刷和印刷速度较慢等限制。优化后的SMMF可以在磁场控制下游动于狭窄的微网络中。Wang等[202]则提出了一个能够在微弱旋转磁场作用下游动并遵循复杂轨迹的、基于MOF的螺旋微机器[图2（e）]。位于结构最外层的沸石咪唑骨架-8（ZIF-8）涂层为药物的包埋提供了一种解决方案，并能够在弱酸性条件下实现药物释放。

一些研究聚焦于对pH刺激反应的材料和异质结构。Hu等[203]模拟了基于pH响应水凝胶的植物系统动态行为用于4D打印，提高了MPL的精度并增强了材料对外部刺激的响应性。他们还通过MPL重建了一个笼状结构，能够抓取物体用于药物递送。Wei等[204]制造了一个具有可逆膨胀特性的pH响应微观结构，并利用BSA材料实现了1.08~2.71的膨胀比，从而为药物递送提供了替代解决方案。Li等[205]设计了一种一次性且单材料捕获结构，可用于多步骤pH响应结构和多种材料的成型。该结构有潜力用于细胞操作和药物递送。

此外，还有基于温度响应的药物释放系统。Zhou等[206]利用聚*N*-丙烯酰基甘氨酸酰胺（PNAGA）制备微机器人，该机器人能够在45 ℃条件下快速溶解并释放药物。

因此，PNAGA被认为是人体内药物输送的有前景的候选材料。然而，正常体温范围较窄，需要开发具有高灵敏度的温度响应型药物递送/释放系统，使其能够在正常体温（约37 ℃）附近快速释放药物。因此，未来的给药机器人在材料选择和结构设计方面还需要进一步优化。

N-异丙基丙烯酰胺（NIPAAm）及其改性物质是保温/光响应软材料中用于光响应药物释放的代表材料。例如，单壁碳纳米管作为分离纤维并入NIPAAm和*N*-二甲基丙烯酰胺（DMAAM）的混合凝胶系统中。它们充当分子储存库，储存DOX作为碱并在酸性环境中释放药物[207]。为了实现微机械在低驱动阈值下的快速响应，Deng等[208]介绍了一种4D打印策略，可用于制造用于药物输送的微型设备。此外，Bozuyuk等[209]制造了一个双螺旋微型游泳器，利用外部光刺激来释放化疗药物DOX。通过用于控制释放剂量的受控光模式来停止药物释放，进一步促进了药物递送在精准医学中的应用。

为了进一步优化载药微型机器人的设计原理/结构，对药物释放进行了建模。Do等[169]首先证明了可以通过修改MPL参数（如孵化距离、切片距离和载体的孔径大小）来控制模式药物释放时间。一般来说，增加的间距会导致更高的药物释放速率，而较小的间距会导致一些遮挡，防止介质渗透，从而导致荧光团释放减少。他们的研究为MPL制造药物输送载体铺平了道路。

总体而言，当前基于MPL制备的微机器人仍主要处于体外实验阶段。未来，需要开展更多严格的体内动物实验，并逐步向临床转化。

（2）微针：微针被广泛用于药物、疫苗和大分子递送，监测与诊断，疾病治疗以及美容等场景[210–211]。MPL具备极高的制造精度和重复性，可以制备几何结构复杂的微针阵列；微针正逐渐被应用于众多生物医学场景。近年来，微针已成为双光子微纳制造中最具有代表性的应用之一。

微针在内耳等精细组织的药物递送方面的表现尤其突出。Yu等[210]与Aksit等[212]使用IP-S光刻胶制备微针阵列，用于豚鼠圆窗膜（RWM）打孔实验，证明了其在内耳疾病药物递送中的可行性；Chiang等[213]在冷冻人体组织上验证了双光子打印微针能够精确在RWM上打孔，展示了其在人类内耳疾病治疗中的潜力。目前已经提出了多种制造方法，用于小批量生产微针，以便将其进一步应用于内耳的药物输送治疗中。Aksit等[214]开发了一种结合了TPL与电化学沉积技术的混合式增材制造方法，制备了高精度、超锐利、金涂层的高精度微针[图2（f）]；Balmert等[215]则提出一种可溶解的倒刺型微针制备方法，结合了MPL和微成形方法，克服了模型工艺的众多难点，实现多成分、多药物疫苗经皮递送[图2（g）]。

除了穿孔给药外，直接经皮给药也可使用微针。在这种对加工精度要求严格的工艺中，针尖或侧开槽上会开小孔。微针前端或侧壁常须开孔或构建开放微流道。Ebrahiminejad等[216]结合MPL与热压复制技术，开发了适用于大批量生产的经皮微针阵列[图2（h）]；为简化微针制造，Faraji Rad等[217]先通过MPL制备具有开放微流道的微针原型[图2（i）]，再利用热塑性复制实现规模化生产，目前已经提出了多种制造方法用于小批量生产微针，以便将其进一步应用于内耳的药物输送治疗中。Faraji Rad等[218]制造出了极其精细的微针并系统研究了扫描速度、激光功率、填充间距、拼接与切片距离等MPL参数对微针结构质量的影响[图2（j）]，为个性化微针设计提供了参数指南。

此外，将微针与微流控芯片集成已成为扩展其应用前景（如生物分子检测等）的重要方向，相关内容将在诊断章节中介绍。

4.1.2. 细胞递送

除了药物，细胞本身也是一种重要的治疗载荷，须实现精准递送[219]。近年来，细胞疗法在再生医学中备受关注[220]，而MPL为设计微纳尺度细胞载体提供了重要工具[221]。Li等[187]制备了刺球状多孔微机器人，能够在体内携带并释放细胞，用于再生医学与细胞疗法[图2（k）]。此外，作者证明了微型机器人的磁驱动能力和细胞携带能力通过模拟和体外实验得到了提升。他们还展示了微型机器人在裸体小鼠体内释放特定部位细胞的能力。这些初步结果支持了利用磁力驱动微型机器人进行体内定向递送细胞的可行性。Jeon等[222]设计了磁驱支架型微机器人，用于干细胞在实验室体外、动物体外与体内的精确递送与移植[图2（l）]，并通过旋转磁场提高其推进效率与可控性。该设计提升了细胞容量。此外，旋转磁场策略提高了细胞在体内流体环境中的推进效率和可控性。

然而，开发用于动物模型中跟踪微型机器人的体内成像技术和制造3D可降解微型机器人仍然充满挑战。Dong等[223]提出了一种集成多功能的软微游泳器，既能承载神经细胞并在体内降解，又可通过磁电刺激诱导神经细胞分化[图2（m）]，他们使用GelMA作为底材，并将$CoFe_2O_4$@$BiFeO_3$（CFO@BFO）核心-壳体磁电纳米颗粒用于微型游泳器，GelMA作为细胞递送过程中生长的良好基础，磁电纳米颗粒则作为磁性运动成分并诱导神经元

细胞的分化。此外，在磁刺激下进行了体外微型机器人降解实验和神经细胞诱导分化实验，展示了此类设计在治疗中枢神经系统（CNS）疾病中的潜力。Wei等[224]设计出一种可磁驱动、影像引导且可降解的微机器人，实现工程化干细胞在原位肝肿瘤中的精准递送，并在裸鼠身上进行了体内实验。实验过程中，可降解微型机器人在目标位点释放了所加载的细胞；四周后，肿瘤生长明显被抑制，表明负荷细胞已被有效递送到感染区域。这是首批在血管组织中展示可降解微机器人靶向细胞递送与疗效的工作之一。

未来，MPL将继续作为蜂窝传输工具，特别是针对性投放。动物体内长期靶向治疗实验可以通过微纳制造各种功能和生物材料实现，包括多阶段驱动控制、细胞释放和生物降解。

4.2. 微组织建模

为了为再生医学提供更多治疗工具，我们需要更深入地理解细胞或微组织与体外环境之间的相互作用[225–226]。在这一背景下，大量研究开始聚焦于微组织的构建。MPL能在微纳米尺度上构建形貌复杂的结构，因此被广泛用于构筑具有生理相关性的微纳米尺度组织，用于疾病建模、体外药物筛选以及组织修复或替代[227]。

4.2.1. 药物筛选与疾病建模

由于缺乏从2D细胞模型向临床转化的有效技术，药物发现仍然十分昂贵。因此，研究人员提出构建工程化细胞系统，以提高筛选数据与临床患者真实反应之间的相关性。对于精准医疗而言，需要建立“患者/个体特异性”的模型，来深入理解药物与个体微组织之间的相互作用[227]。然而，此类模型需要个性化的微结构。人体组织在几何形貌上存在显著差异，具有从宏观到纳米尺度的多尺度几何特征。MPL能以高分辨率构建3D复杂结构，并打印体外细胞支架或微结构，因此被广泛用来制备用于药物筛选和疾病建模的微结构及微阵列。

“器官芯片”（organ-on-chips, OoC）是疾病建模、药物与毒性筛选等生物医学应用中的理想工具[228–229]。通过MPL制备的OoC已被广泛用于构建血-脑屏障（BBB）模型、心脏疾病模型以及其他器官或组织模型。Marino等[230]首次提出了一种1∶1比例的3D仿生杂化BBB模型，用于研究纳米材料穿越BBB的过程，以服务脑疾病的治疗与诊断。该模型由连接结构、交汇处以及带孔或不带孔的毛细血管构成，采用IP-DiLL（Nanoscribe, Germany）作为光刻材料。在该模型中，多孔管状结构模拟了脑微血管的结构与功能。芯片制备完成后，将bEnd.3内皮细胞接种在多孔微毛细血管周围，然后将芯片与外部泵系统连接，形成约1 mm·s^{-1}的液体流速，接近体外生理条件。该系统为研究纳米材料与药物穿越BBB提供了理想平台。Tricinci等[231]也制备了一个1∶1比例的3D真实仿生脑肿瘤微环境模型，用于CNS疾病的高通量药物筛选[图3（a）]。在该模型中，内皮细胞hCMEC/D3均匀分布于管腔内部空间，而星形胶质细胞与U87胶质母细胞瘤（GB）细胞培养于外部空间。当构建GB微环境时，研究者采用抗体功能化的穆替林负载纳米结构脂质载体，评估其在用于肿瘤治疗的药物负载纳米颗粒中对渗透性的影响。这项研究加速了针对脑癌及多种神经退行性疾病的新型治疗策略的发展[232]。然而，利用MPL在中尺度到毫米尺度范围内制备多重结构，通常需要多步骤打印，耗时以“天”为量级。因此，目前在这类模型中，往往仅利用MPL制造微纳米级别的关键结构。

除了BBB模型之外，MPL也被用于心脏芯片的制备。Michas等[233]构建了一个由人诱导多能干细胞（iPSC）来源的心肌细胞（hiPSC-CM）驱动的集成微流体系统，在芯片上复现了心室功能[图3（b）]。该系统模拟了由微型超材料支架支撑的心室腔室、心脏瓣膜以及对抗压差的单向流动。支架与瓣膜采用IP-S光刻胶并通过MPL制备。

肝组织药物筛选也是一个重要方向。Zeußel等[234]利用MPL构建了模拟肝小叶微形貌的支架，实现流体灌注[图3（c）]。模拟结果表明，该支架中的剪切应力、流速和流线与天然肝小叶相当，表明MPL在未来体外肝脏药物筛选中具有潜力。Zhang等[235]采用动态多焦MPL工艺并行制备微阵列，通过全息预设计结合透镜相位调制生成多束飞秒激光焦点，大幅提升了微结构制备效率。构建的支架可作为阵列分析平台，用于揭示所载药物的抗癌效果。

为了更好理解微环境与细胞之间的相互作用，许多研究者利用MPL制备细胞支架。Tayalia等[236]首先通过MPL制备了具有不同横向孔径的细胞培养支架，并研究了人纤维肉瘤细胞系在其中的行为。Barin等[237]利用MPL制备了体外胶瘤细胞支架，能够保持上皮生长因子受体高表达以及细胞微管网络结构的特性，从而更好地用于癌细胞活动研究与后续药物筛选[图3（d）]。Rengaraj等[238]通过MPL设计微尺度支架，并在其表面涂覆生物活性薄膜，以模拟转移性癌症早期发展阶段[图3（e）]。涂层由HA和聚-*L*-赖氨酸构成，可调节刚度，并加载纤连蛋白及骨形态发生蛋白2和4（BMP2和BMP4）等基质结合蛋白。研究者还考察了胰腺癌细胞（PANC1和PAN092）在多层聚电解质膜（PEM）上的黏附与生长情

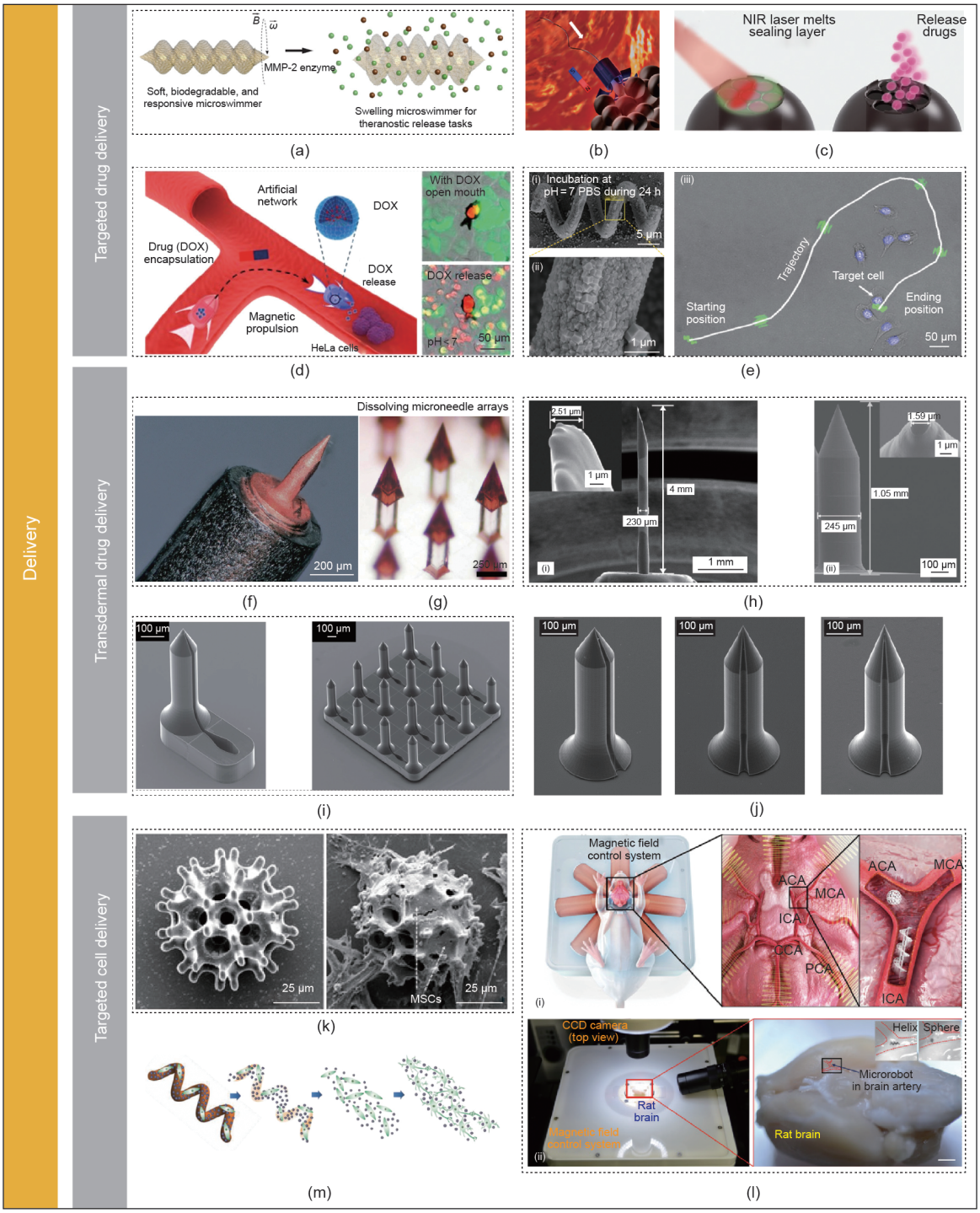

图2. MPL在给药系统中的应用。（a）3D打印的可降解螺旋微机器人及其在旋转磁场中的驱动示意图。*B*：磁感应强度；*w*：磁场角速度；MMP-2：基质金属蛋白酶-2。经许可转载自参考文献[114]。（b）精子-杂交微马达实现的靶向药物递送示意图。经许可转载自参考文献[195]。（c）仿马勃菌（puffball）微机器人药物释放过程示意图。经许可转载自参考文献[196]。（d）形变微游泳体（SMMF）的磁推进及多柔比星（DOX）释放过程示意图。经许可转载自参考文献[200]。DOX释放过程[（e-i）、（e-ii）]以及基于金属-有机骨架的生物医用微机器人（MOFBOTS）的运动示意图（e-iii）。经许可转载自参考文献[202]。（f）通过MPL制备的可注射递药微结构的光学显微照片。经许可转载自参考文献[214]。（g）用于多组分皮肤疫苗接种的可溶解倒刺型（下切）微针阵列。经许可转载自参考文献[215]。（h）商用BD Ultra-Fin™ 4 mm胰岛素笔针（Franklin Lakes, New Jersey, USA）（h-i）与热塑性Zeonor 1060R（Zeon, Japan）复制件（h-ii）的比较。经许可转载自参考文献[216]。（i）带有开放式微流道的热塑性微针阵列扫描电镜（SEM）图像。经许可转载自参考文献[217]。（j）聚合物微针阵列的SEM图像。经许可转载自参考文献[218]。（k）用于靶向细胞递送的磁性微机器人SEM图像。MSCs：间充质干细胞。经许可转载自参考文献[187]。（l）在体外对大脑中的微型机器人进行磁性驱动。（l-i）离体脑血管模型及磁场控制系统示意图；（l-ii）用于磁力操控的实验装置以及一只大脑结构清晰（血管可见）且被固定住的大鼠。带透明血管的离体脑模型。ICA：颈内动脉；ACA：前大脑动脉；MCA：中大脑动脉；CCA：颈总动脉；PCA：后大脑动脉；CCD：电荷耦合器件相机。（l-ii）的比例尺为2 mm。经许可转载自参考文献[222]。（m）载有细胞的软质微泳器在磁场作用下的降解过程，以及SH-SY5Y细胞在磁场刺激下发生神经元分化的情况。经许可转载自参考文献[223]。

况，证明了生物活性 PEM 可以沉积在支架上。该研究为在更长时间尺度上开展癌细胞调控和抑制肿瘤生长的药物治疗研究提供了有用证据，并表明通过 MPL 在微尺度设计支架是可行路径。

尽管 MPL 能在一定程度上模拟部分细胞生长环境的微结构，但关于细胞-环境相互作用的效应（如流体剪切力）仍然缺乏系统研究。为了进一步发展疾病模型并开展更可靠的体外药物筛选，未来研究需要更多关注微结构的功能化，同时在体外模拟流体环境，以获取有关药物筛选结果可靠性的关键信息。

4.2.2. 组织/细胞支架与组织修复/替代

再生医学的终极目标是通过构建人工替代物来维持并增强人体组织功能[239]，实现这一目标的关键在于精准构建 3D 人类组织模型。传统 3D 打印主要在宏观尺度进行，并不适合微纳米制造。因此，人们引入 MPL 进行微纳米尺度制造，从而加速了诸如微型支架和细胞“壁龛”（niches）等小尺度工具的应用[240–242]。这些支架类器件可以逐步精确模拟 3D 细胞 ECM，实现从成分到结构、从空间分布到时间分布的模拟构建[243–244]。此外，在支架表面涂覆蛋白可以用来研究生物相容性、细胞迁移、细胞形态与细胞力学[236,245–246]。

除了单一材料的细胞支架外，基于 MPL 的异质细胞支架也被用于研究 ECM 诱导的细胞生长[247–248]。Richter 等[247]采用 MPL 结合三种不同光刻胶（蛋白排斥型光刻胶、蛋白黏附型光刻胶以及可光活化的钝化光刻胶），并在其上功能化接枝不同 ECM 蛋白，从而设计了用于细胞培养的 3D 支架[图 3（f）]。他们提出了一种构建多蛋白功能化 3D 微环境的策略，可以更准确地在微观尺度复制微组织 ECM 的空间分布。通过引入 lockyballs 等新工具，定向自组装也被引入再生医学，用于产生脂肪干细胞（ASC）球形团块，从而增强再生效果[249–250]。Ovsianikov 等[251]利用 MPL 制备了用于组织工程的 3D 支架，并研究了支架材料 PEGDA 的空间分辨率与照射参数之间的关系，同时考察了不同 PI 类型、不同浓度与支架细胞毒性之间的关系。这些工作为制备在物理与生物属性上均类似原生细胞环境的 3D 支架提供了指导。

在骨组织构建及相关免疫调控方面，研究人员投入了大量努力。通过 MPL 制备的微型支架被用于构建多种细胞组织（包括骨组织）。在这类设计中，MPL 所用光刻胶必须可降解且对细胞无毒，这大大限制了可用于制备微型支架的材料选择[252–254]。Terzaki 等[255]将利用 MPL 制备的 3D 支架与自组装、具有钙结合能力的肽结合使用，结果表明随着细胞增殖增加，细胞黏附显著增强，矿化程度也明显提高，此策略有望用于硬组织工程。Koroleva 等[256]利用 MPL 制备了用于自体骨组织工程的 3D Zr-Si 支架[图 3（g）]。他们考察了不同孔径支架的力学性能、干细胞接种效率、细胞增殖以及向成骨谱系分化的诱导效果。Timashev 等[257]制备了以 PLA 为基体的支架，其杨氏模量可与人骨相当。该 PLA 支架在体外为成骨 MSC 分化提供了有利微环境，并支持体外骨再生。Mihailescu 等[258]采用激光辅助技术制备了骨组织工程用成骨细胞接种结构，其中包含三角晶格排列的垂直微管阵列。研究表明，这些结构在植入造血干细胞后有良好的骨再生效果和成骨潜力，为骨组织修复提供了另一类备选方案。Felfel 等[259]使用聚（*D*,*L*-乳酸-共-*ε*-己内酯）（PLCL）共聚物、丝弹蛋白样重组水凝胶以及纳米-HA 构建多相混合支架用于骨修复。不过，此类支架在高分辨率与高通量之间存在权衡，限制了其临床应用。Weisgrab 等[260]首次通过 MPL 在宏观尺度制备了高度多孔、可降解且生物相容的组织工程支架[图 3（h）]。Nouri-Goushki 等[261]设计了六种不同高度的微柱，用于观察巨噬细胞极化。这些结果有望用于今后探索与亚微米表面形貌相关的骨免疫调节现象，对骨科植入物的制造具有参考意义。

总之，基于 MPL 的微组织是研究再生医学的重要工具。然而，由于 ECM 成分的复杂性、几何结构的多样性、生化信号空间分布的差异以及其他未知因素，目前这些微组织仍无法直接用于临床实践。

4.3. 手术

微型器件系统已成为精准手术的一种有前景的解决方案，并大大扩展了外科医生的操作能力[262]。此外，用于制造这些微器件的激光本身，在手术过程中也可以充当“锋利的手术刀”。因此，通过 MPP 制备的微器件，有望在未来为精细手术提供一整套“工具箱”。

4.3.1. 光动力治疗（PDT）

PDT 是一种微创技术，在临床实践中被广泛应用，尤其是用于各种癌症（如前列腺癌、乳腺癌、头颈部肿瘤、皮肤癌、胰腺癌和肺癌）的检测与治疗[263–265]。在 PDT 中，首先将 PS 递送至肿瘤组织。在光照激发下，肿瘤细胞会产生活性氧（ROS），从而诱导细胞凋亡，杀死靶向肿瘤细胞或其他病原体[265]。为了提高 PDT 的治疗效果，需要主要考虑三个因素：PS、光源以及分子氧[266–267]。与 UV/VIS 相比，NIR 光在生物组织中的穿透更深；再结合具有高 ROS 产生效率并在 NIR 区有吸收的

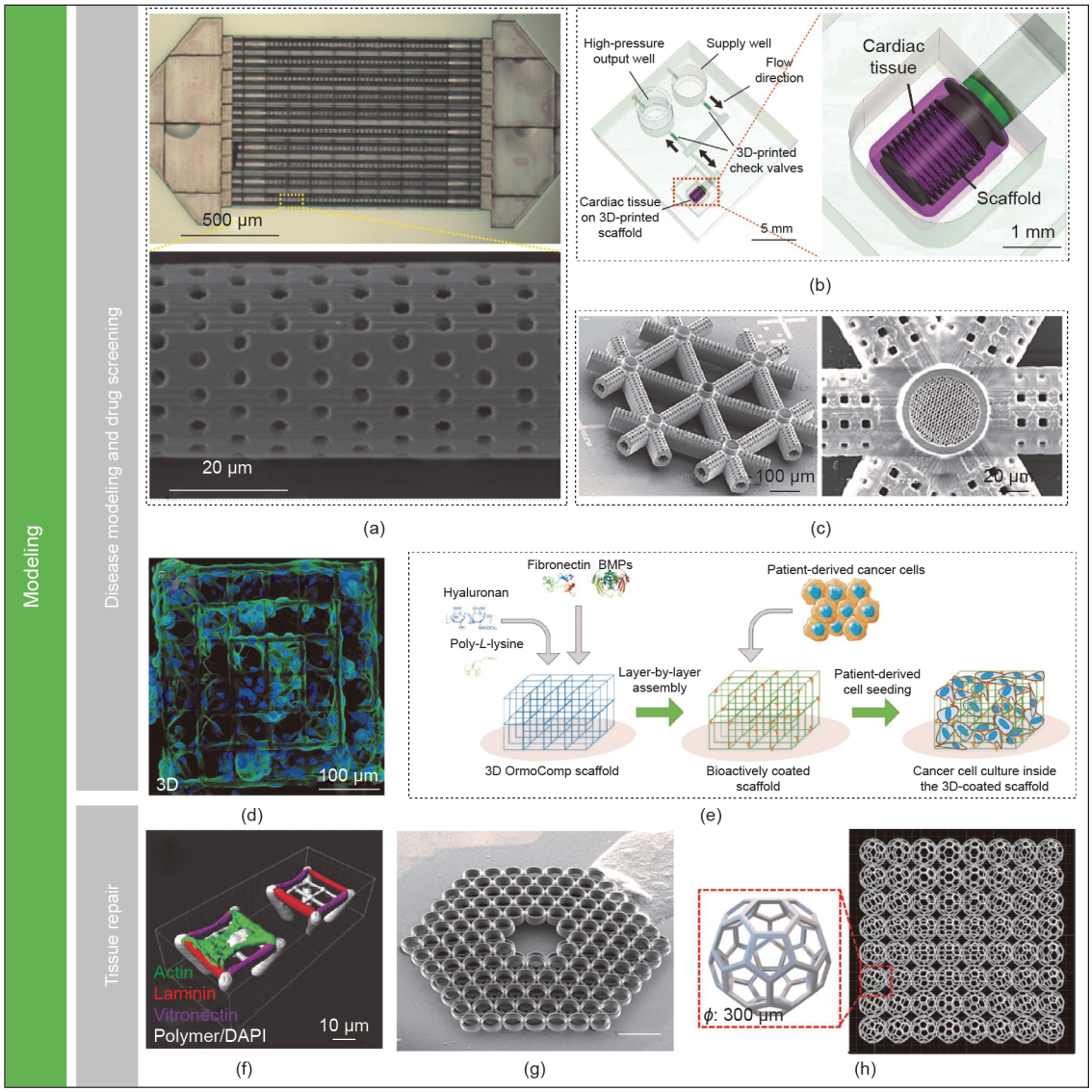

图3. MPL在微组织建模中的应用。（a） 血-脑屏障（BBB）仿生结构的SEM图像。经许可转载自参考文献[231]。（b）微型超材料支架支撑的收缩心肌腔室示意图。经许可转载自参考文献[233]。（c） 基于SU-8的肝组织仿生微结构SEM图像，经许可转载自参考文献[234]。（d）基于3D支架构建的多细胞共培养组织模型示意图。经许可转载自参考文献[237]。（e）转移性癌症早期发展阶段的示意图以及利用3D微结构支架模拟转移过程的策略。经许可转载自参考文献[238]。（f）激光扫描显微镜（LSM）采集的3D图像重建结果，覆盖整个微结构高度；示意肺癌A549细胞（细胞核为白色）优先黏附在涂覆层黏连蛋白的梁上。DAPI：4',6-二脒基-2-苯基吲哚，用于细胞核染色。经许可转载自参考文献[247]。（g）有机-无机复合支架的SEM图像。比例尺为500 μm。经许可转载自参考文献[256]。（h）基于巴基球（buckyball）的3D支架设计示意图。φ：巴基球直径。经许可转载自参考文献[260]。

PS，使得双光子激发PDT（TPE-PDT）在近十年得到了快速发展。

2008年，Starkey等[268]首次报道基于PS的PDT能够在肿瘤细胞上引起一定程度的肿瘤组织退缩。这一结果激发了研究者去设计具有高效率、低毒性的PS，并在此基础上将成像手段引入双光子动态治疗。例如，Guo等[269]开发了一种多模态聚合物纳米颗粒（PNP）。这种纳米颗粒可用于双光子荧光成像以及TPE-PDT [图4（a）]技术，成为实现细胞成像、深层组织成像以及高效PDT的理想候选材料。此外，Wu等[80]开发了基于碳点（CD）的PDT系统。该系统具备荧光成像、线粒体靶向和双光子诱导5-氨基酮戊酸（5-ALA）释放能力，具体步骤如下。首先，通过将ALA与香豆素连接合成了光触发材料。随后，将靶向线粒体化合物三苯基膦（TPP）和CD加入衍生物中，形成纳米系统（CD-ALA-TPP）。在PDT期间，纳米系统优先积累于线粒体中释放5-ALA，在氧化作用下对癌细胞造成双光子照射损伤[图4（b）]。他们的研究提出了一种副作用较小的PDT使用新策略。Dobos等[93]利用3D骨肉瘤细胞培养开发了TPE-PS（即P2CK、嗜红Y和卟啉衍生物）的体外筛选平台[图4（c）]。Huang等[270]结合TPA荧光共振能量转移和单分子胶束的NIR光热效应，提升了现有PS的治疗效率[图4（d）]。

然而，与单光子PDT相比，TPE-PDT的ROS较低，能够高效杀死目标肿瘤细胞。不过，有些PS可以产生更高的ROS。因此，高ROS产生与TPA提升之间的矛盾仍未解决，未来研究应予以解决。

4.3.2. 微操控

微操控（如细胞的捕获与固定）是单细胞治疗与分析中的关键技术[271–273]。能够执行微操作的微型器件有望成为未来精准手术的重要工具。

Alapan等[274]设计了一种形状编码的动态移动微机器组装体，在外加磁场驱动旋转时，可沿螺旋螺纹方向实现垂直运输，从而实现微尺度物体在3D空间中的运输与操控，为精准微操控提供了一种潜在策略。Ma等[161]设计了由两种不同材料构成的复杂微型机器人：以相对刚性的SU-8作为骨架以及以柔性pH响应型蛋白作为“智能肌肉”机器人。这些异质结构微机器人能够以良好可控的方式抓取并释放微小物体。Hu等[275]采用基于组装的制备策略，构建了3D形变磁性软结构（微驱动器），可应用于可重构的细胞外基质中，用于操控易损的微尺度物体。Jia等[179]制备了由分子马达组装体驱动的3D打印蛋白基机器人结构，提出了一种新的微操纵器制造策略，例如，能够在激活后实现抓取和摆动的微型手和微型臂[图4（e）]。Wang等[276]开发了一种受捕蝇草启发的3D水凝胶驱动器，其运动可通过pH变化进行调控[图4（f）]，能够实现微物体的抓取与释放。此外，还可采用不同的释放策略，对多个微物体的释放行为进行精确控制，实现同步或依次释放。这些研究结果展示了微尺度软驱动器在生物医学工程中实现精准操控的巨大潜力。微注射是精准手术中的另一项重要技术。Yagoub等[277]开发了一种用于简化胞质内单精子注射（ICSI）的微型器件，该器件由两个微尺度组件组成：舱体（pod）和基座（garage）[图4（g）]；细胞被放置在舱体中，并停靠于基座内。该研究为高通量微注射提供了一种易于实现的策略。

4.3.3. 细胞分选

细胞分选是生物医学领域的一项关键工具，用于从复杂、异质的混合物中纯化悬浮细胞[278–279]。由于TPP具备制备微结构的能力，其已被应用于微流控系统中的被动细胞分选（主要可分为膜基分选和柱基分选）。

Wang和Papautsky [280]设计了一种基于尺寸的微流控多模式微粒分选器，提高了样品分离效率，并拓展了惯性微流控在复杂微粒样品分选中的应用范围。Xu等[281]提出了一种新型拱形微分选器，可实现微粒的多模式分选（即高捕获、带状捕获和低捕获模式）。该设计不仅使微分选器在前端与后端分选尺寸上能够以灵活且精确的方式进行调节，还降低了长期使用中的堵塞问题。其性能通过从人血中富集SUM 159三阴性乳腺肿瘤细胞得到验证，显示出在循环肿瘤细胞分离和血细胞分选等应用中的潜力。Perrucci等[282]设计了一种膜基微流控过滤系统，成功将TPP制备的悬浮式微滤器集成到3D打印的微流控结构中。该系统采用尺寸可控的荧光微粒进行评估，表明其在细胞分选方面具有应用潜力。Zhang等[283]提出了一种交叉流分选器，通过具有不同狭缝尺寸的微柱对不同尺寸的微粒进行分级分离。这类分选器同样可用于细胞分选。

Hu等[284]制备了一种用于微粒与细胞操控的可调微流控器件（TMFD）。微环阵列中的pH响应水凝胶通过TPP集成到TMFD中，可在pH变化时于200 ms内实现快速膨胀与收缩。通过调节pH值，TMFD能够对特定尺寸（5~10 μm）的微粒进行多级过滤与捕获[图4（h）]。Kaynak等[285]基于水凝胶制备了一种多体机械系统，可通过超声换能实现频率选择性的驱动，用于显微尺度取样。该系统由“μ-jet”发动机、收集腔和筛网组成[图4（i）]。当发动机在其共振频率下被周期性激励时，可输运携带细胞的流体，随后细胞在收集腔中被收集，并通过筛网在目标尺寸范围内完成过滤。Wang等[286]制备了一种磁驱动旋转式微滤器，可在微流控芯片内实现过滤模式与通过模式之间的切换[图4（j）]。这些多模式过滤功能进一步拓展了其在复杂混合物细胞分选中的应用。

4.4. 诊断

微器件是疾病诊断的有前景的工具[8,287–289]，因其能特异性识别生理信号或靶向分子（包括细胞、细菌、蛋白质和离子）的作用因子，而这些生物标志物或生物信号可用于癌症、感染等疾病的临床分析与诊断。

4.4.1. 生物信号检测

生物信号传感与检测作为精准医疗的诊断环节至关重要，而精准的生物信号传感更有利于实现个性化医疗诊断[271,290]。因此，许多通过MPL技术制造的微阵列已被应用于生物医学领域。AI-Abaddi等[291]将MPL与传统光刻技术相结合，成功制备出用于生物信号检测的3D聚合物电极[图5（a）]。Haque等[292]在二氧化硅基底上设计了桥柱结构，该结构通过3D打印并部分碳化处理。研究展示了碳化聚合物电极作为低成本、兼容CMOS的单片式生物传感器平台在疾病诊断与治疗中的潜力。然而，该装置采用刚性玻璃或二氧化硅基底，限制了其长期植入应

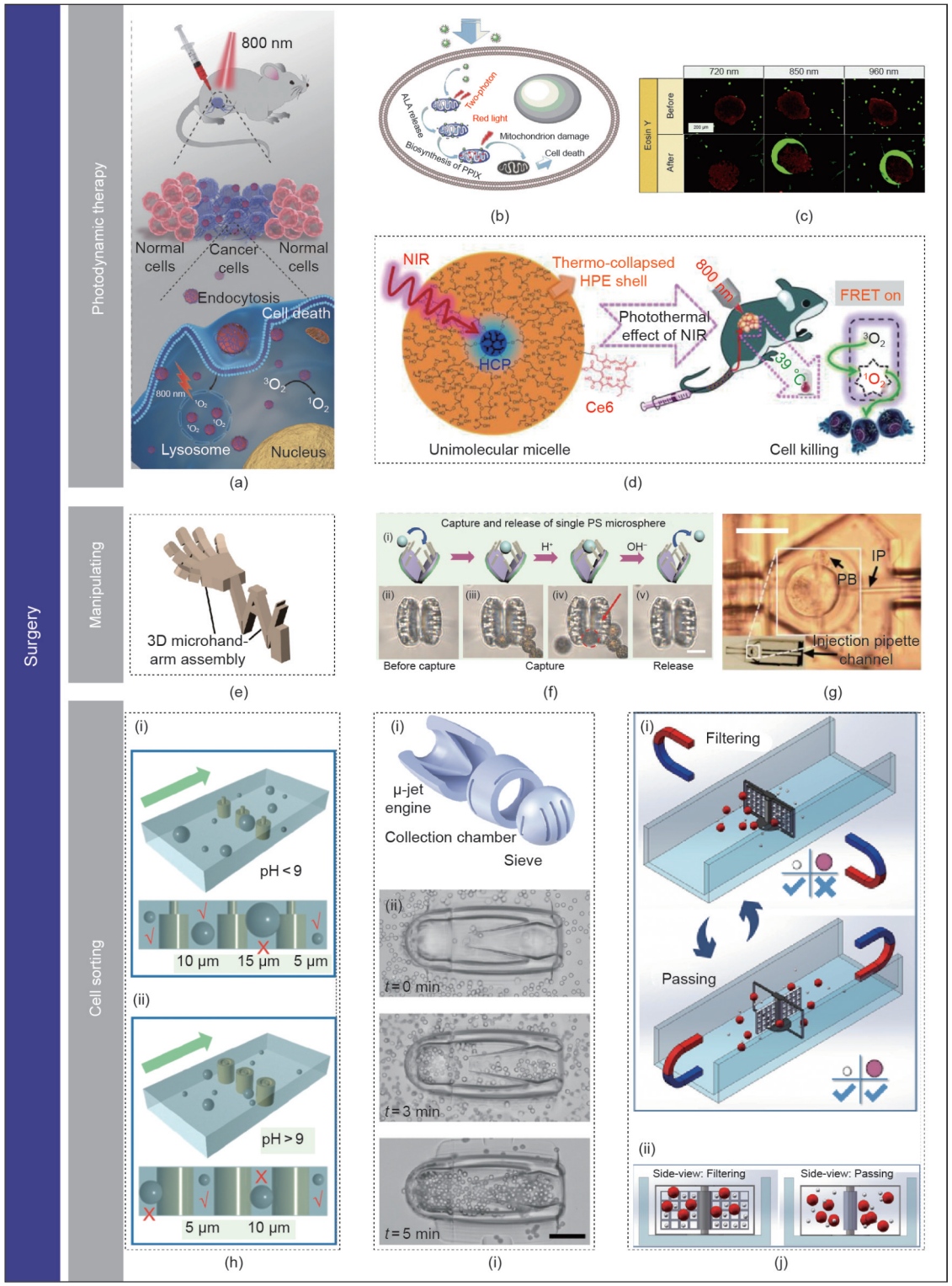

图4. MPL在精准手术中的应用。（a）体内双光子激发光动力治疗（TPE-PDT）的示意图。经许可转载自参考文献[269]。（b）对癌细胞产生促凋亡作用的过程示意图。PPIX：原卟啉 IX。经许可转载自参考文献[80]。（c）TPE-PDT 处理的 mCherry 标记 MG63 球状体（红色），其周围环绕着表达凋亡相关斑点样蛋白并与 CARD 结构域相关的绿色荧光蛋白（ASC-GFP）标记单细胞（绿色）。比例尺为 200 μm。经许可转载自参考文献[93]。（d）NIR 照射与 TPE-PDT 在体外产生光热效应的示意图。HCP：超支化共轭聚合物；HPE：超支化聚醚；Ce6：叶绿素 e6，商业光敏剂（PS）；FRET：荧光共振能量转移。经许可转载自参考文献[270]。（e）机械臂的示意图。经许可转载自参考文献[179]。仿生水凝胶微执行器的微球捕获与释放行为示意图（f-i），以及捕捉行为前（f-ii）、捕获 PS 微球[（f-iii）、（f-iv）]和释放行为后（f-v）的仿生微结构的图像。比例尺为 10 μm。经许可转载自参考文献[276]。（g）用于卵母细胞（oocyte）操作的 3D 微夹持和储存结构（“pod”与“garage”）示意图及其显微图像。比例尺为 120 μm。PB：极体；IP：注射针管。经许可转载自参考文献[277]。（h）TMFD 在 pH < 9（h-i），pH > 9（h-ii）时进行三粒级颗粒过滤程序的示意图。经许可转载自参考文献[284]。用于颗粒收集和分选的微流控装置示意图（i-i）及颗粒收集实验结果（i-ii）。比例尺为 75 μm。经许可转载自参考文献[285]。磁性控旋转微滤器以过滤颗粒的示意图（j-i）及各模式下的侧视示意（j-ii）。经许可转载自参考文献[286]。

用。为解决这一问题，Brown等[51]开发了一种高长宽比微电极阵列。该电极阵列集成在薄膜柔性电缆上，适用于鸣禽等小型动物的神经记录[图5（b）]。因此，将MPL与薄膜制备工艺相结合，可有效解决阵列微型化及高长径比结构制造等难题，为精密测试提供支持。然而，慢性植入物功能缺失的问题引发了安全性和生物相容性方面的担忧。Abu Shihada等[293]创新性地将MPL与薄膜技术融合，成功研制出新型高度可定制的3D微电极阵列。该微电极阵列为研究正常生理状态及各类病理条件下的神经活动提供了独特研究平台[图5（c）]。展望未来，若MPL微器件应用于生物信号传感领域，特别是植入式生物传感系统，其核心挑战将在于如何确保植入材料的生物相容性[1]。

4.4.2. 生物标记物检测

除了电生理信号外，蛋白质和离子等众多生物标志物也可用于精准疾病诊断。许多研究已采用MPL制造能准确检测这类生物标志物的诊断设备。Miller等[294]开发了首款微针离子选择性电极（ISE）装置，用于测量生理相关钾离子浓度[图5（d）]。他们使用多孔碳和多孔石墨烯电极测试了ISE的换能器，结果显示多孔碳钾离子ISE的检测范围为10^{-5}~10^{-2} mol·L^{-1}，近似能斯特斜率为每十倍程57.9 mV，且能在约20 S内快速稳定。因此，ISE作为体表传感器监测钾离子水平的平台颇具吸引力，可潜在应用于即时检测（POC）场景。Miller等[295]基于ISE装置的设计理念，提出将单针实时检测平台与多功能管上管电极阵列相结合的远程自动化诊断方案，可检测多种相关生物标志物。研究还聚焦于将蛋白质作为生物标志物进行检测。Wollhofen等[296]开发了一种由两种丙烯酸聚合物构成的3D检测平台，该平台通过链霉亲和素-生物素相互作用和抗体识别高密度脂蛋白（HDL）颗粒中载脂蛋白A1的两种检测方法进行验证。该平台有望应用于芯片式流动细胞仪，实现3D多重检测分析。Trautmann等[297]则展示了一种创新的混合检测方案。该研究通过飞秒激光辐照与加热技术，将微针与微流体通道及MPL技术相结合[图5（e）]。这套微流控系统可应用于即时诊断中的微流控注射与采血操作。Suzuki等[298]通过仿生设计，成功制备出用于采血的中空微针结构。

科研人员还致力于细菌生物标志物的检测研究。Li等[299]开发了一种基于MPL与石墨烯的增强型生物传感平台，可检测运动细菌及酒窖代谢物[图5（f）]。该装置能

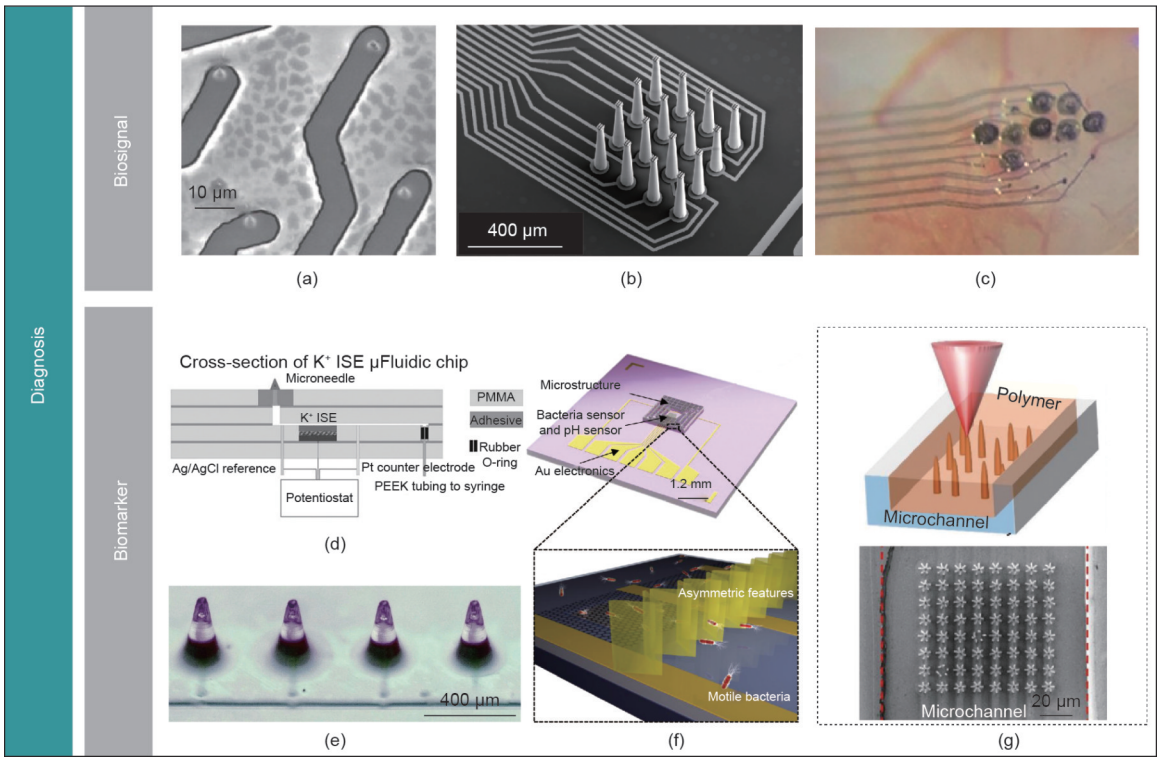

图5. MPL在诊断工具制备中的应用。（a）3D打印微结构电极的SEM图像。经许可转载自参考文献[291]。（b）用于神经信号记录的微电极阵列SEM图像。经许可转载自参考文献[51]。（c）微电极阵列体内小鼠记录。经许可转载自参考文献[293]。（d）钾离子选择电极（K^+ ISE）微流控芯片的截面示意图；Pt：铂电极；PEEK：聚醚醚酮基底；PMMA：聚甲基丙烯酸甲酯。经许可转载自参考文献[294]。（e）用于即时（POC）诊断的微流控系统示意图。经许可转载自参考文献[297]。（f）。一种用于检测细菌浓度的生物传感器。经许可转载自参考文献[299]。（g）用于表面增强拉曼散射（SERS）检测的嵌入微结构的微流道示意图及其应用。经许可转载自参考文献[300]。

及时诊断细菌感染，从而降低并发症发生率和死亡率。Lao等[300]开发了一种可切换的自组装方法，用于制备3D纳米间隙等离子体结构，实现微流控表面增强的拉曼光谱（SERS）传感[图5（g）]。他们将超临界干燥技术与毛细管力驱动的MPL微柱自组装工艺相结合。这些微通道中的纳米结构实现了抗癌药物的检测，展示了其用于精准医疗领域原位监测的潜力。

5. 结论、挑战与展望

5.1. 结论

MPL是一种强大的3D激光微纳制造方法，已在化学、材料科学、生物医学和机械工程等多个学科受到广泛关注。它能够以极高精度塑造几何形貌复杂的结构，使其成为生物医学领域极具价值的工具。与挤出打印等传统生物制造技术相比，各类“非接触式”方法（包括MPL）在制造过程中更易维持无菌环境，这是生物医学应用的前提条件。与其他光敏制造方法（如SLA和DLP）相比，MPL拥有更高的制造精度，可在微纳米尺度上构建复杂结构。

总的来说，在微纳米尺度上设计和制造诊疗工具，是精准医疗的重要发展方向。过去十年中，双光子纳米制造技术已被广泛应用于精准医疗中的多个场景，包括药物和活细胞递送、用于替代和药物筛选的微组织建模、用于精准手术的手术工具以及用于诊断的生物信号与生物标志物传感器等（表4）[294,301–303]。在这些应用场景中，靶向给药与经皮给药是目前最具发展前景的研究方向，有望通过动物实验进一步优化生物材料结构、药物释放特性、剂量与给药方式。然而，由于PI、光聚合材料、MPP低通量以及实用化优化等多方面因素的限制，这些方法目前仍无法直接用于临床应用。

5.2. 挑战与机遇

5.2.1. 材料：生物安全性、力学性能与功能性

在临床应用中，确保微型器件或精准医疗治疗手段的安全性是首要且基础的前提条件[304]。治疗的安全性与材料的生物相容性和生物可降解性密切相关，尤其与PI和光聚合物的生物安全性息息相关。

此外，水是生物体内的基本溶剂。水溶性材料更容易与机体内环境相互作用，从而减轻对组织的刺激和不良反应；同时，也更易在体液作用下实现降解与代谢。因此，在面向生理环境设计PI时，保证其水溶性至关重要。在精准医疗中，为提升双光子微纳制造的制备效率，人们希望采用既高效又具良好生物相容性的PI。然而，水溶性发色团和PI通常表现出较差的聚合效率，使得PI的设计与合成长期以来一直是MPL领域的一大挑战。因此，这类PI的设计与合成目前仍是研究热点。

与合成材料相比，天然材料在用于光聚合时往往具有更好的生物相容性。但天然材料的力学性能通常不如合成材料优异。基于此，研究者正积极合成天然材料的衍生物，以同时赋予材料良好的力学性能与生物相容性。这些衍生物有望应用于长期诊断类器件中。

多种功能材料（如刺激响应型、超弹性以及异质材料等）也已被深入研究。通过开发多样化的功能材料并优化其特定性质（如pH响应性、收缩速率等），可以为微尺度工具的制备提供更多可行方案。此外，杂化材料也被用于双光子微纳制造：在制备过程中掺入功能材料，以赋予最终结构特定系统所需的性质，如较强的磁驱动能力或优异的光响应性能。

综上，在材料的合成设计中需要重点考虑三个方面：用于保障生物安全性的生物材料、用于使力学性能与目标需求相匹配的结构材料以及用于为精准医疗装备提供功能解决方案的功能材料。

5.2.2. 工艺：高效率与高分辨率

尽管在现有微纳制造技术中，MPL具备高精度和高结构复杂度等优势，但其打印速度较慢，限制了其在生物医学应用中实现大规模制备。目前，人们正从工艺角度对MPL进行改进，包括进一步提升制造效率和打印精度。本文简要回顾了近年来已被部分解决的工艺局限，并对未来应如何应对这些挑战提出了技术性展望。

为提高制备速度，研究人员对加工流程进行了优化。Geng等[305]在MPL中引入了随机寻址的数字微镜器件扫描系统，在不牺牲分辨率的前提下实现了22.7 kHz的高制备速度，并展示了一种用于大规模纳米成型和构筑复杂结构的策略。Saha等[306]采用了类似策略，与串行MPL系统相比，在保持亚微米分辨率的前提下，使制备速率提高了2~3个数量级，其体积加工速率也超过20 $mm^3 \cdot h^{-1}$。Ouyang等[307]开发了一种基于数字全息的TPL平台，通过最多2000个可单独编程的激光焦点实现并行打印，以90 nm的分辨率制备复杂的3D结构。

除了从光路设计层面提升MPL的加工效率外，自动化质量控制和可打印性优化也正逐步被引入。Lee等[308]利用机器学习模型加速光剂量参数的寻优过程，并实现了零部件质量的自动检测。他们提出通过视频监测MPL中

表4　通过 MPL 制备的典型生物医学应用器件

Type	Devices/application	Structure	Materials (functionality)	Innovations	Ref.
Delivery systems	Microrobots/cargo delivery	Helical	Photoresist: LAP + GelMA/poly(ethylene glycol) amine MMP-2 enzyme degradation: GelMA Magnetic actuation: Fe_3O_4 MNPs	Enhance the release of embedded cargo molecules	[114]
	Microrobots/cargo delivery	Heterogeneous and SMMF	Photoresist: EMK + DPEHA/TEA/ NIPAAm/AAc/PVP pH stimulus: AAc	Provide ideal platforms for complex microcargo operations and on-demand drug release	[200]
	Microrobots/cargo delivery	Helical	Photoresist: IP-L (Nanoscribe, Germany) Magnetically control: Ni-coated Biocompatible and degradation: Ti-coated Characteristics in low PH value (6): ZIF-8	Achieve single-cell targeting in a cell culture media and a controlled delivery of cargo payloads inside a complex microfluidic channel network	[202]
	Microrobots/drug delivery	Puffball	Photoresist: IP-S (Nanoscribe) Biocompatible: Ti sputtering Magnetically control: Ni-coated Sealing layer: PCL diol-IR780 NIR stimulus	Replicate the unique characteristics of puffball fungi, such as high spore payloads and protection of payload, via the barrier cap	[196]
	Microrobots/drug delivery	Helical and bacterial flagellar-like	Photoresist: GelMA + P2CK Endocytosis of drugs into cells: FA Magnetically control: Fe@ZIF-8	Improve the drug transportation ability of microrobots	[199]
	Microrobots/drug delivery	Fish-inspired structure (skeleton, head, and body)	Photoresist: LAP + GelMA/PEG Skeleton: Fe_3O_4 MNPs embedded in PEGDA Head and body: GelMA	Provide a multidrug delivery method for targeted therapy	[197]
	Microrobots/drug delivery	Helix	Photoresist: P2CK + PNAGA/PEGDA-575 Magnetically control: Fe@ZIF-8 Thermosensitive: PNAGA	Provide a robust pathway to the development of high-performance thermosensitive hydrogel-based microrobots	[206]
	Microrobots/cell delivery	Conical hollow microhelices	Photoresist: EMK + SZ2080 Biocompatible: Ti sputtering Magnetic actuation: Ni-coated	Improve the capability of swimming and decrease the lateral drift	[194]
	Microrobots/cell delivery	Helical/spherical and scaffold-type	Photoresist: IP-Dip (Nanoscribe) Biocompatible: Ti sputtering Magnetically control: Ni-coated	Develop magnetically actuated scaffold-type microrobots as a platform for precise stem cell delivery and transplantation *in vitro*, *ex vivo*, and *in vivo*	[222]
	Microrobots/cell delivery	A burr-like porous spherical structure	Photoresist: SU-8 Biocompatible: Ti sputtering Magnetically control: Ni-coated	Provide a micro-robotic device platform for regenerative medicine and cell-based therapy	[187]
	Microrobots/vaccine delivery	Spherical	Photoresist: (1) GelMA microrobots: LAP + GelMA (2) Skeleton core: parbenate + PEGDA/PETA/Fe_3O_4 MNPs + 2-isopropylthioxanthone	Provide an efficient vaccination strategy by controlling the expression duration of DNA vaccines	[301]
	Microneedles/inner ear delivery	Diameter of 100 μm, length of 150 μm, a tip radius of curvature of 500 nm	Photoresist: IP-S	Create a temporary microperforation in the RWM without causing significant anatomic or physiologic dysfunction	[210]
Microtissue modeling	Scaffolds in a chip/ drug screening	Two sets of fine flexible concentric helices	Photoresist: IP-Dip	Replicate the ventricular function on a chip	[233]
	OoCs/drug screening	Microtubes inspired by the brain capillaries	Photoresist: IP-S	Capable of hindering dextran diffusion through the bioinspired BBB	[230]
	OoCs/drug screening	Microtubes inspired by the brain capillaries	Photoresist: IP-DiLL (Nanoscribe)	Effective formation of a bioinspired cellular barrier based on microtubes that reproduce brain microcapillaries to scale	[231]

续表

Type	Devices/application	Structure	Materials (functionality)	Innovations	Ref.
Microtissue modeling	Scaffolds/drug screening	Microcage array	Photoresist: EMK + AAc Crosslinker: PETA	Real cellular responses to dynamic 3D microenvironments can be investigated	[235]
	Scaffolds/cell-migration study	Woodpile	Photoresist: Lucirin TPO-L (BASF, Germany)+ SR368/SR499 (Arkema Sartomer, France)	Find that the 3D environment produces higher cell speeds than a 2D substrate	[236]
	Scaffolds/bone repair	Star-shaped	Photoresist: acrylated polylactide	Scaffolds pre-seeded with MSCs provided a beneficial microenvironment for osteogenesis and bone regeneration *in vitro* and *in vitro*	[257]
	Scaffolds/bone repair	Buckyball	Photoresist: PTMC-based resin	Prove that repetitive units on the macro scale can be produced	[260]
	Scaffolds/retina repair	—	Photoresist: IP-S	Produce autologous retinal cell grafts that represent a promising therapeutic approach for those suffering from late-stage retinal degeneration	[302]
	Scaffolds/neuronal implants	—	Photoresist: EMK + 4-arm acrylated PLA	Reveal good biocompatibility of the material-based scaffolds	[138]
Diagnosis	Electrodes/neural recording	A 16-channel array of 350 μm tall electrodes with a 20 μm diameter at the recording tip	Photoresist: OrmoComp (micro resist technology, Germany)	Provide new tools for high-density neural recording	[51]
	Biosensor/bacteria sensing	A cage comprising a venous valve-inspired directional microstructure	Photoresist: IP-S (Nanoscribe, Germany) Functionalization of pH sensor and bacteria sensors: graphene-based	Bacteria-concentrating effect shows a 3.38–3.5-fold enhancement	[299]
	POC system/micro-fluidic injection and extraction	Microfluidic channels and microneedles	Photoresist: OrmoComp (micro resist technology, Germany)	Simplify the fabrication process of creating a microfluidic system with microneedles	[297]
	Microneedle ISE sensor/measuring the K^+ concentrations	Microfluidic system and microneedles	Photoresist: Eshell 300 (Envision Tec, Germany)	The first demonstration of a microneedle ISE sensor	[294]
	3D platform/protein assay	With binding pins	Photoresist: Irgacure 819 + PETA/CEA/PEGDA	A simplified approach for HDL protein profiling	[296]
Surgery	Nanosystem/PDT	—	CD-ALA-TPP	A new strategy for PDT with lesser side effects	[80]
	Microactuator/ microscopic manipulation	Bionic asymmetric structure	Photoresist: TPO/HMPP + DMAEMA/PEGDA/ PETA	Realize the simultaneous and successive release and multiobject capture	[276]
	Micromachine/ OoCs manipulations	Spherical	Photoresist: LAP + PNIPAAm/AAc Magnetic actuation: Fe_3O_4-doped Crosslinker: BIS	Show the multiresponsive behavior as a powerful approach for precisely targeted obstructive interventions and OoC manipulations	[303]
	Microfluidic system/cell sorting	Microring array integrated into microfluidic device	Photoresist: EMK + PNIPAAm/AAc/DPEPA/TEA	Realize multifiltering and complete trapping of particles and cells without external devices	[284]
	Micromachine/cell selecting and sorting	Comprised of a μ-jet engine, a collection chamber, and a sieve	Photoresist: EMK/Irgacure 369 + PEGDA/PETA	Realize acoustic actuation cell sorting	[285]

BIS: *N*, *N*′-methylenebis-acrylamide; CEA: 2-carboxyethylacrylate; DMF: *N*, *N*-dimethylformamide; DMSO: dimethyl sulfoxide; DPEHA: dipentaerythritol hexaacrylate; DPEPA: dipentaerythritol pentaacrylate; EL: ethyl lactate; EMK: 4,4′-bis(diethylamino) benzophenone; MNPs: magnetic nanoparticles; Irgacure 819: phenylbis(2,4,6-trimethylbenzoyl)phosphine oxide; IR780: 2-[2-[2-chloro-3-[(1,3-dihydro-3,3-dimethyl-1-propyl-2*H*-indol-2-ylidene)ethylidene]-1-cyclohexen-1-yl]ethenyl]-3,3-dimethyl-1-propylindolium iodide; Lucirin TPO-L: ethyl (2,4,6-trimethylbenzoyl)phenylphosphinate; MBAA: *N*, *N*′-methylene bisacrylamide; MMP-2: matrix metalloproteinase 2; parbenate: ethyl 4-(dimethylamino)benzoate; PLA: polylactide; PTMC: poly(trimethylene-carbonate); PVP: polyvinylpyrrolidone; SR368: tris(2-hydroxyethyl)isocyanurate triacrylate; SR499: ethoxylated (6) trimethylolpropane triacrylate; TPO: diphenyl(2,4,6-trimethylbenzoyl) phosphine oxide.

不同结构的加工过程，对已固化、未固化、损伤、照射等状态进行分类监控与过程控制，模型分类准确率达到95.1%。Pingali和Saha [309]构建了基于机器学习的代理模型，用于预测面投影式双光子（P-TPL）打印性能，从而可快速而智能地选择光刻胶及打印参数。Jia等[310]提出了一种物理机理引导与数据驱动相结合的混合建模框架，用于预测和提升MPL中的几何精度。该通用方法对半径和高度的平均预测误差分别为5.23%和4.66%。此外，其补偿策略将半径的几何误差从22.19%降低至3.21%，将高度误差从12.18%降低至4.96%。

许多研究还聚焦于提升打印分辨率。体素尺寸决定了MPL的空间分辨率，因为它同时受聚合特性以及焦点处光子密度分布与曝光条件的影响。基于这些认识，Wang等[311]在次阈值曝光条件下，使用IP-Dip光刻胶制备出了特征尺寸小于10 nm的悬空纳米线。为克服高度方向像差和激光吸收导致的激光功率衰减问题，Tan等[312]采用了激光功率补偿策略，从而提升了MPL的成形精度。通过引入灰度控制[313–315]，打印复杂度也得到了进一步增强。现有工作主要集中在优化MPL的打印效率和分辨率，而这些指标在众多微纳制造方法中同样需要综合权衡与优化。

对于微组织建模及其他异质微结构的构筑，则必须采用多材料微纳打印。Mayer等[316]在MPL装置中引入了微流控系统，用于实现多材料3D微纳制造。然而，这些改进仍须在生物医学应用场景下进一步验证。总之，MPL未来面临的最关键挑战仍是其低通量问题。为解决这一难题，一个潜在方案是将DLP与MPL相结合，这将需要在装置层面进一步集成DLP与MPL系统。

5.2.3. 应用：稳定性与成本

从应用角度来看，大多数用于精准医疗的多光子成型纳米器件仍处于前期探索阶段。其中许多器件仅在体外或体内对其相应功能进行了验证。在药物递送、疾病模型构建、外科手术和诊断这四类应用场景中，药物递送系统最具前景；然而，它们在材料与结构设计之间需要更加平衡的考量。尽管具体应用各不相同，功能材料通常被用作药物释放的“开关”，而生物材料若要用于MPL，则必须考虑其生物降解特性。不过，对于组织工程支架而言，需要首要考量的未必是生物降解特性，而是严格且长期的生物相容性。此外，药物递送系统对精度的要求也不必达到外科微操作工具的同一水平。微组织建模、外科手术工具和诊断工具则需要具备更高功能性、更佳生物相容性以及更精细结构设计的材料。因此，有必要基于双光子聚合在材料与结构设计方面开展进一步研究。多光子微纳制造在未来实际应用中所面临的主要挑战是稳定性和成本。从应用成熟度来看，靶向递送器件最为领先；然而，由于动物实验数量有限，其进一步发展受到制约。若要在临床环境中大规模应用多光子微纳制造并优化相关器件，就必须开展大量动物实验。传统多光子制造工艺通量较低，而动物模型成本高昂，这使得整个过程既耗资又耗时。目前，用于精准医疗的许多双光子成型微纳器件仍停留在概念模型阶段，其在未来人体模型中的功能稳定性有待进一步验证。

MPL器件成本的一部分来自飞秒激光光源，这在一定程度上限制了其规模化。近年来，许多研究人员致力于探索新的光聚合微纳3D打印机理，以替代传统MPL。Sanders等[317]采用三态融合上转换机理实现3D打印。值得注意的是，该技术仅需4 mW的连续波激发即可工作，降低了设备成本。Hahn等[318]在苯偶姻中引入两步吸收机制，以此取代TPA作为3D激光纳米打印中的基础光引发机理，在降低MPL成本的同时实现了亚微米级精度。然而，其打印速度仍然非常缓慢。在此基础上，Hahn等[319]提出了一种称为光片3D激光微打印的方法，将图像投影与基于双色两步吸收的逻辑与型光学非线性相结合。因此，在体素体积为0.55 μm^2的条件下，实现了7×10^6体素·s^{-1}的峰值打印速度。在一定程度上，这些研究推动了激光微纳3D打印设备的降本与普及。然而，由于生物医学应用在光学性能方面对材料有着极为严格的要求，这些技术在生物医学领域的应用目前仍然面临挑战。未来，如果能借助连续激光技术来实现MPA和器件制备，则有望大幅降低MPL在生物医学领域应用的成本。

上述研究结果极大拓展了我们关于双光子微纳制造在生物医学应用方面的设想。随着在微纳尺度上对材料特性、结构设计和工艺优化的进一步探索，包括精准医疗在内的众多生物医学应用场景将逐步得以实现。

CRediT authorship contribution statement

Jiarui Hu: Writing-original draft. An Ren: Data curation, Conceptualization. **Weikang Lv:** Data curation, Conceptualization. **Abdellah Aazmi:** Data curation, Conceptualization. **Changwei Qin:** Data curation, Conceptualization. **Xinyi Liang:** Data curation, Conceptualization. **Xiaobin Xu:** Writing-review & editing, Conceptualization. **Mengfei Yu:** Writing-review & editing,

Conceptualization. **Qi Li:** Writing-review & editing, Conceptualization. **Huayong Yang:** Supervision, Resources. **Liang Ma:** Writing-review & editing, Supervision, Resources, Conceptualization.

Declaration of competing interest

The authors declare that they have no known competing financial interests or personal relationships that could have appeared to influence the work reported in this paper.

致谢

作者感谢国家重点研发计划（2018YFA0703000）和国家自然科学基金（52275294）的资助。

References

[1] Guzzi EA, Tibbitt MW. Additive manufacturing of precision biomaterials. Adv Mater 2020;32(13):1901994.
[2] Xiong Y, Kang H, Zhou H, Ma L, Xu X. Recent progress on microfluidic devices with incorporated 1D nanostructures for enhanced extracellular vesicle (EV) separation. Biodes Manuf 2022;5(3):607–16.
[3] Lin Z, Jiang T, Shang J. The emerging technology of biohybrid micro-robots: a review. Biodes Manuf 2022;5(1):107–32.
[4] Mazzoli A. Selective laser sintering in biomedical engineering. Med Biol Eng Comput 2013;51(3):245–56.
[5] Yang M, Yang L, Peng S, Deng F, Li Y, Yang Y, et al. Laser additive manufacturing of zinc: formation quality, texture, and cell behavior. Biodes Manuf 2023;6(2):103–20.
[6] Isaacson A, Swioklo S, Connon CJ. 3D bioprinting of a corneal stroma equivalent. Exp Eye Res 2018;173:188–93.
[7] Greant C, Van Durme B, Van Hoorick J, Van Vlierberghe S. Multiphoton lithography as a promising tool for biomedical applications. Adv Funct Mater 2023;33(39):2212641.
[8] Soto F, Wang J, Ahmed R, Demirci U. Medical micro/nanorobots in precision medicine. Adv Sci 2020;7(21):2002203.
[9] Aazmi A, Guo ZX, Yu HR, Lv WK, Ji ZC, Yang HY, et al. Enhanced mixing efficiency for a novel 3D Tesla micromixer for Newtonian and non-Newtonian fluids. J Zhejiang Univ Sci A 2023;24(12):1065–78. Chinese.
[10] Zhao DK, Xu HQ, Yin J, Yang HY. Inkjet 3D bioprinting for tissue engineering and pharmaceutics. J Zhejiang Univ Sci A 2022;23(12):955–73. Chinese.
[11] Castilho M, de Ruijter M, Beirne S, Villette CC, Ito K, Wallace GG, et al. Multitechnology biofabrication: a new approach for the manufacturing of functional tissue structures? Trends Biotechnol 2020;38(12):1316–28.
[12] Harley W, Yoshie H, Gentile C. Three-dimensional bioprinting for tissue engineering and regenerative medicine in down under: 2020 Australian workshop summary. ASAIO J 2021;67(4):363–9.
[13] Moroni L, Boland T, Burdick JA, De Maria C, Derby B, Forgacs G, et al. Biofabrication: a guide to technology and terminology. Trends Biotechnol 2018; 36(4):384–402.
[14] Ma L, Yang H. What's next toward the bio-design and manufacturing field? Biodes Manuf 2023;6(6):735–41.
[15] Sun Y, Yu K, Gao Q, He Y. Projection-based 3D bioprinting for hydrogel scaffold manufacturing. Biodes Manuf 2022;5(3):633–9.
[16] Rajabasadi F, Schwarz L, Medina-Sánchez M, Schmidt OG. 3D and 4D lithography of untethered microrobots. Prog Mater Sci 2021;120:100808.
[17] Faraji Rad Z, Prewett PD, Davies GJ. High-resolution two-photon polymerization: the most versatile technique for the fabrication of microneedle arrays. Microsyst Nanoeng 2021;7(1):71.
[18] Liao C, Wuethrich A, Trau M. A material odyssey for 3D nano/microstructures: two photon polymerization-based nanolithography in bioapplications. Appl Mater Today 2020;19:100635.
[19] Göppert-Mayer M. About elementary acts with two quantum jumps. Ann Phys 1931;401(3):273–94. German.
[20] He GS, Tan LS, Zheng Q, Prasad PN. Multiphoton absorbing materials: molecular designs, characterizations, and applications. Chem Rev 2008;108(4): 1245–330.
[21] Kaiser W, Garrett CGB. Two-photon excitation in CaF_2: Eu^{2+}. Phys Rev Lett 1961;7(6):229–31.
[22] Maruo S, Kawata S. Two-photon-absorbed near-infrared photopolymerization for three-dimensional microfabrication. J Microelectromech Syst 1998; 7(4): 411–5.
[23] Butkus A, Skliutas E, Gailevičius D, Malinauskas M. Femtosecond-laser direct writing 3D micro/nano-lithography using VIS-light oscillator. J Cent South Univ 2022;29(10):3270–6.
[24] Skliutas E, Lebedevaite M, Kabouraki E, Baldacchini T, Ostrauskaite J, Vamvakaki M, et al. Polymerization mechanisms initiated by spatio-temporally confined light. Nanophotonics 2021;10(4):1211–42.
[25] Ladika D, Butkus A, Melissinaki V, Skliutas E, Kabouraki E, Juodkazis S, et al. X-photon 3D lithography by fs-oscillators: wavelength-independent and photoinitiator-free 2023. Light Adv Manuf 2024;5(4):567–79.
[26] Zhao Y, Luo H, Liang Z, Deng M, Duan X. Micro-nano 3D printing based on photopolymerization and its development status and trends. Chinese J Laser 2022;49(10):1002703. Chinese.
[27] Kuebler SM, Rumi M, Watanabe T, Braun K, Cumpston BH, Heikal AA, et al. Optimizing two-photon initiators and exposure conditions for three-dimensional lithographic microfabrication. J Photopolym Sci Technol 2001;14(4):657–68.
[28] Kuebler SM, Braun KL, Zhou W, Cammack JK, Yu T, Ober CK, et al. Design and application of high-sensitivity two-photon initiators for three-dimensional microfabrication. J Photochem Photobiol A 2003;158(2–3):163–70.
[29] Pucher N, Rosspeintner A, Satzinger V, Schmidt V, Gescheidt G, Stampfl J, et al. Structure–activity relationship in D-π-A-π-D-based photoinitiators for the two-photon-induced photopolymerization process. Macromolecules 2009; 42(17):6519–28.
[30] Fischer J, Wegener M. Three-dimensional direct laser writing inspired by stimulated-emission-depletion microscopy. Opt Mater Express 2011;1(4):614.
[31] Liu T, Tao P, Wang X, Wang H, He M, Wang Q, et al. Ultrahigh-printing-speed photoresists for additive manufacturing. Nat Nanotechnol 2023;19(1):51–7.
[32] Yu H, Ding H, Zhang Q, Gu Z, Gu M. Three-dimensional direct laser writing of PEGda hydrogel microstructures with low threshold power using a green laser beam. Light Adv Manuf 2021;2(1):31–8.
[33] Cantoni F, Maher D, Bosler E, Kühne S, Barbe L, Oberschmidt D, et al. Round-robin testing of commercial two-photon polymerization 3D printers. Addit Manuf 2023;76:103761.
[34] Mueller P, Thiel M, Wegener M. 3D direct laser writing using a 405 nm diode laser. Opt Lett 2014;39(24):6847.
[35] Li L, Fourkas JT. Multiphoton polymerization. Mater Today 2007;10(6):30–7.
[36] Xiao P, Zhang J, Dumur F, Tehfe MA, Morlet-Savary F, Graff B, et al. Visible light sensitive photoinitiating systems: recent progress in cationic and radical photopolymerization reactions under soft conditions. Prog Polym Sci 2015;41: 32–66.
[37] Pennacchio FA, Fedele C, De Martino S, Cavalli S, Vecchione R, Netti PA. Three-dimensional microstructured azobenzene-containing gelatin as a photoactuable cell confining system. ACS Appl Mater Interfaces 2018; 10(1): 91–7.
[38] Baudis S, Bomze D, Markovic M, Gruber P, Ovsianikov A, Liska R. Modular material system for the microfabrication of biocompatible hydrogels based on thiol-ene-modified poly(vinyl alcohol). J Polym Sci A Polym Chem 2016; 54(13):2060–70.
[39] Park SH, Lim TW, Yang DY, Kim RH, Lee KS. Improvement of spatial resolution in nano-stereolithography using radical quencher. Macromol Res 2006;14(5):559–64.
[40] Harinarayana V, Shin YC. Two-photon lithography for three-dimensional fabrication in micro/nanoscale regime: a comprehensive review. Opt Laser Technol 2021;142:107180.
[41] Huang Z, Chi-Pong Tsui G, Deng Y, Tang CY. Two-photon polymerization nanolithography technology for fabrication of stimulus-responsive micro/nano-structures for biomedical applications. Nanotechnol Rev 2020;9(1):1118–36.
[42] Lu J, Sun M, Zhang J, Yang X, Dong M, He H, et al. Benidipine-loaded nanoflower-like magnesium silicate improves bone regeneration. Biodes Manuf

2023;6(5):507–21.
[43] Bunea AI, del Castillo IN, Droumpali A, Wetzel AE, Engay E, Taboryski R. Micro 3D printing by two-photon polymerization: configurations and parameters for the nanoscribe system. Micro 2021;1(2):164–80.
[44] Olsen MH, Hjortø GM, Hansen M, Met Ö, Svane IM, Larsen NB. In-chip fabrication of free-form 3D constructs for directed cell migration analysis. Lab Chip 2013;13(24):4800–9.
[45] O'Halloran S, Pandit A, Heise A, Kellett A. Two-photon polymerization: fundamentals, materials, and chemical modification strategies. Adv Sci 2023; 10(7):2204072.
[46] Srinivasaraghavan Govindarajan R, Sikulskyi S, Ren Z, Stark T, Kim D. Characterization of photocurable IP-PDMS for soft micro systems fabricated by two-photon polymerization 3D printing. Polymers (Basel) 2023;15(22):4377.
[47] Serien D, Takeuchi S. Multi-component microscaffold with 3D spatially defined proteinaceous environment. ACS Biomater Sci Eng 2017;3(3):487–94.
[48] Haas KH, Wolter H. Synthesis, properties and applications of inorganic-organic copolymers (ORMOCER®s). Curr Opin Solid State Mater Sci 1999;4(6):571–80.
[49] Emmert K, Amberg-Schwab S, Braca F, Bazzichi A, Cecchi A, Somorowsky F. bioORMOCER®—compostable functional barrier coatings for food packaging. Polymers 2021;13(8):1257.
[50] Ovsianikov A, Chichkov B, Adunka O, Pillsbury H, Doraiswamy A, Narayan R. Rapid prototyping of ossicular replacement prostheses. Appl Surf Sci 2007; 253(15):6603–7.
[51] Brown MA, Zappitelli KM, Singh L, Yuan RC, Bemrose M, Brogden V, et al. Direct laser writing of 3D electrodes on flexible substrates. Nat Commun 2023; 14(1):3610.
[52] Malinauskas M, Danilevičius P, Baltriukienė D, Rutkauskas M, Zukauskas A, Kairytė Ž, et al. 3D artificial polymeric scaffolds for stem cell growth fabricated by femtosecond laser. Lith J Phys 2010;50(1):75–82.
[53] Mačiulaitis J, Deveikytė M, Rekštytė S, Bratchikov M, Darinskas A, Šimbelytė A, et al. Preclinical study of SZ2080 material 3D microstructured scaffolds for cartilage tissue engineering made by femtosecond direct laser writing lithography. Biofabrication 2015;7(1):015015.
[54] Maciulaitis J, Rekštytė S, Bratchikov M, Gudas R, Malinauskas M, Pockevicius A, et al. Customization of direct laser lithography-based 3D scaffolds for optimized *in vivo* outcome. Appl Surf Sci 2019;487:692–702.
[55] Conci C, Jacchetti E, Sironi L, Gentili L, Cerullo G, Osellame R, et al. A miniaturized imaging window to quantify intravital tissue regeneration within a 3D microscaffold in longitudinal studies. Adv Opt Mater 2022;10(7):2101103.
[56] Sackmann EK, Fulton AL, Beebe DJ. The present and future role of microfluidics in biomedical research. Nature 2014;507(7491):181–9.
[57] Abgrall P, Conedera V, Camon H, Gue AM, Nguyen NT. SU-8 as a structural material for labs-on-chips and microelectromechanical systems. Electrophoresis 2007;28(24):4539–51.
[58] Seet KK, Juodkazis S, Jarutis V, Misawa H. Feature-size reduction of photopolymerized structures by femtosecond optical curing of SU-8. Appl Phys Lett 2006;89(2):024106.
[59] Tottori S, Zhang L, Qiu F, Krawczyk KK, Franco-Obregón A, Nelson BJ. Magnetic helical micromachines: fabrication, controlled swimming, and cargo transport. Adv Mater 2012;24(6):811–6.
[60] Kim S, Qiu F, Kim S, Ghanbari A, Moon C, Zhang L, et al. Fabrication and characterization of magnetic microrobots for three-dimensional cell culture and targeted transportation. Adv Mater 2013;25(41):5863–8.
[61] Suter M, Zhang L, Siringil EC, Peters C, Luehmann T, Ergeneman O, et al. Superparamagnetic microrobots: fabrication by two-photon polymerization and biocompatibility. Biomed Microdevices 2013;15(6):997–1003.
[62] Peters C, Ergeneman O, García PDW, Müller M, Pané S, Nelson BJ, et al. Superparamagnetic twist-type actuators with shape-independent magnetic properties and surface functionalization for advanced biomedical applications. Adv Funct Mater 2014;24(33):5269–76.
[63] Wloka T, Gottschaldt M, Schubert US. From light to structure: photo initiators for radical two-photon polymerization. Chen Eur J 2022;28(32):e202104191.
[64] Cumpston BH, Ananthavel SP, Barlow S, Dyer DL, Ehrlich JE, Erskine LL, et al. Two-photon polymerization initiators for three-dimensional optical data storage and microfabrication. Nature 1999;398(6722):51–4.
[65] Jhaveri SJ, McMullen JD, Sijbesma RP, Tan LS, Zipfel WR, Ober CK. Direct three-dimensional microfabrication of hydrogels via two-photon lithography in aqueous solution. Chem Mater 2009;21(10):2003–6.
[66] Xing J, Liu L, Song X, Zhao Y, Zhang L, Dong X, et al. 3D hydrogels with high resolution fabricated by two-photon polymerization with sensitive water soluble initiators. J Mater Chem B 2015;3(43):8486–91.
[67] Balta DK, Arsu N. Host/guest complex of β-cyclodextrin/5-thia pentacene-14-one for photoinitiated polymerization of acrylamide in water. J Photochem Photobiol Chem 2008;200(2–3):377–80.
[68] Xing J, Liu J, Zhang T, Zhang L, Zheng M, Duan X. A water soluble initiator prepared through host–guest chemical interaction for microfabrication of 3D hydrogels via two-photon polymerization. J Mater Chem B 2014;2(27):4318–23.
[69] Carmona T, Cañeque T, Custodio R, Cuadro AM, Vaquero JJ, Mendicuti F. Cucurbit[n]urils as a potential fine-tuned instrument for modifying photophysical properties of D-π-A^+-π-D "push-pull" chromophores. Dyes Pigments 2014;103: 106–17.
[70] Zheng YC, Zhao YY, Zheng ML, Chen SL, Liu J, Jin F, et al. Cucurbit[7]uril-carbazole two-photon photoinitiators for the fabrication of biocompatible three-dimensional hydrogel scaffolds by laser direct writing in aqueous solutions. ACS Appl Mater Interfaces 2019;11(2):1782–9.
[71] Gao W, Chao H, Zheng YC, Zhang WC, Liu J, Jin F, et al. Ionic carbazole-based water-soluble two-photon photoinitiator and the fabrication of biocompatible 3D hydrogel scaffold. ACS Appl Mater Interfaces 2021;13(24):27796–805.
[72] Malinauskas M, Žukauskas A, Bičkauskaitė G, Gadonas R, Juodkazis S. Mechanisms of three-dimensional structuring of photo-polymers by tightly focussed femtosecond laser pulses. Opt Express 2010;18(10):10209.
[73] Nakayama A, Kumamoto Y, Minoshima M, Kikuchi K, Taguchi A, Fujita K. Photoinitiator-free two-photon polymerization of biocompatible materials for 3D micro/nanofabrication. Adv Opt Mater 2022;10(18):2200474.
[74] Skliutas E, Samsonas D, Čiburys A, Kontenis L, Gailevičius D, Berzinš J, et al. X-photon laser direct write 3D nanolithography. Virtual Phys Prototyp 2023; 18(1):e2228324.
[75] Taguchi A, Nakayama A, Oketani R, Kawata S, Fujita K. Multiphoton-excited deep-ultraviolet photolithography for 3D nanofabrication. ACS Appl Nano Mater 2020;3(11):11434–41.
[76] Crowe JA, El-Tamer A, Nagel D, Koroleva AV, Madrid-Wolff J, Olarte OE, et al. Development of two-photon polymerised scaffolds for optical interrogation and neurite guidance of human iPSC-derived cortical neuronal networks. Lab Chip 2020;20(10):1792–806.
[77] Albota M, Beljonne D, Brédas JL, Ehrlich JE, Fu JY, Heikal AA, et al. Design of organic molecules with large two-photon absorption cross sections. Science 1998;281(5383):1653–6.
[78] Nag OK, Nayak RR, Lim CS, Kim IH, Kyhm K, Cho BR, et al. Two-photon absorption properties of cationic 1, 4-bis(styryl) benzene derivative and its inclusion complexes with cyclodextrins. J Phys Chem B 2010;114(29):9684–90.
[79] Li C, Luo L, Wang S, Huang W, Gong Q, Yang Y, et al. Two-photon microstructure-polymerization initiated by a coumarin derivative/iodonium salt system. Chem Phys Lett 2001;340(5–6):444–8.
[80] Wu H, Zeng F, Zhang H, Xu J, Qiu J, Wu S. A nanosystem capable of releasing a photosensitizer bioprecursor under two-photon irradiation for photodynamic therapy. Adv Sci 2016;3(2):1500254.
[81] Ladika D, Noirbent G, Dumur F, Gigmes D, Mourka A, Barmparis GD, et al. Synthesis and application of triphenylamine-based aldehydes as photo-initiators for multi-photon lithography. Appl Phys A 2022;128(9):745.
[82] Chandler EM, Berglund CM, Lee JS, Polacheck WJ, Gleghorn JP, Kirby BJ, et al. Stiffness of photocrosslinked RGD-alginate gels regulates adipose progenitor cell behavior. Biotechnol Bioeng 2011;108(7):1683–92.
[83] Benedikt S, Wang J, Markovic M, Moszner N, Dietliker K, Ovsianikov A, et al. Highly efficient water-soluble visible light photoinitiators. J Polym Sci A Polym Chem 2016;54(4):473–9.
[84] Bagheri A, Jin J. Photopolymerization in 3D printing. ACS Appl Polym Mater 2019;1(4):593–611.
[85] Engelhardt S, Hoch E, Borchers K, Meyer W, Krüger H, Tovar GEM, et al. Fabrication of 2D protein microstructures and 3D polymer-protein hybrid microstructures by two-photon polymerization. Biofabrication 2011;3(2):025003.
[86] Campagnola PJ, Delguidice DM, Epling GA, Hoffacker KD, Howell AR, Pitts JD, et al. 3-Dimensional submicron polymerization of acrylamide by multiphoton excitation of xanthene dyes. Macromolecules 2000;33(5):1511–3.
[87] Tardivo JP, Del Giglio A, de Oliveira CS, Gabrielli DS, Junqueira HC, Tada DB, et al. Methylene blue in photodynamic therapy: from basic mechanisms to clinical applications. Photodiagn Photodyn Ther 2005;2(3):175–91.
[88] Zeynali A, Marini M, Chirico G, Bouzin M, Borzenkov M, Sironi L, et al. Multiphoton fabrication of proteinaceous nanocomposite microstructures with photothermal activity in the infrared. Adv Opt Mater 2020;8(13):2000584.
[89] Li Z, Torgersen J, Ajami A, Mühleder S, Qin X, Husinsky W, et al. Initiation efficiency and cytotoxicity of novel water-soluble two-photon photoinitiators for direct 3D microfabrication of hydrogels. RSC Advances 2013;3(36):15939–46.
[90] Tromayer M, Dobos A, Gruber P, Ajami A, Dedic R, Ovsianikov A, et al. A biocompatible diazosulfonate initiator for direct encapsulation of human stem

cells via two-photon polymerization. Polym Chem 2018;9(22):3108–17.
[91] Brigo L, Urciuolo A, Giulitti S, Della Giustina G, Tromayer M, Liska R, et al. 3D high-resolution two-photon crosslinked hydrogel structures for biological studies. Acta Biomater 2017;55:373–84.
[92] Ovsianikov A, Mühleder S, Torgersen J, Li Z, Qin XH, van Vlierberghe S, et al. Laser photofabrication of cell-containing hydrogel constructs. Langmuir 2014; 30(13):3787–94.
[93] Dobos A, Steiger W, Theiner D, Gruber P, Lunzer M, Van Hoorick J, et al. Screening of two-photon activated photodynamic therapy sensitizers using a 3D osteosarcoma model. Analyst 2019;144(9):3056–63.
[94] Zhang W, Soman P, Meggs K, Qu X, Chen S. Tuning the poisson's ratio of biomaterials for investigating cellular response. Adv Funct Mater 2013;23(25): 3226–32.
[95] Torgersen J, Ovsianikov A, Mironov V, Pucher N, Qin X, Li Z, et al. Photo-sensitive hydrogels for three-dimensional laser microfabrication in the presence of whole organisms. J Biomed Opt 2012;17(10):105008.
[96] Li Z, Siklos M, Pucher N, Cicha K, Ajami A, Husinsky W, et al. Synthesis and structure-activity relationship of several aromatic ketone-based two-photon initiators. J Polym Sci A Polym Chem 2011;49(17):3688–99.
[97] Carlotti M, Mattoli V. Functional materials for two-photon polymerization in microfabrication. Small 2019;15(40):1902687.
[98] Lodish HF, Berk AJ, Zipursky SL, Matsudaira P, Baltimore D, Darnell J. Collagen: the fibrous proteins of the matrix. Mol Cell Biol 2000;4:145–54.
[99] Xiang L, Cui W. Biomedical application of photo-crosslinked gelatin hydrogels. J Leather Sci Eng 2021;3(1):3.
[100] Olsen D, Yang C, Bodo M, Chang R, Leigh S, Baez J, et al. Recombinant collagen and gelatin for drug delivery. Adv Drug Deliv Rev 2003;55(12):1547–67.
[101] Tytgat L, Dobos A, Markovic M, Van Damme L, Van Hoorick J, Bray F, et al. High-resolution 3D bioprinting of photo-cross-linkable recombinant collagen to serve tissue engineering applications. Biomacromolecules 2020;21(10):3997–4007.
[102] Dulnik J, Kołbuk D, Denis P, Sajkiewicz P. The effect of a solvent on cellular response to PCL/gelatin and PCL/collagen electrospun nanofibres. Eur Polym J 2018;104:147–56.
[103] Yang JR, He HM, Li D, Zhang Q, Xu LZ, Ruan CS. Advanced strategies in the application of gelatin-based bioink for extrusion bioprinting. Biodes Manuf 2023;6(5):586–608.
[104] Qiao Q, Zhang X, Yan Z, Hou C, Zhang J, He Y, et al. The use of machine learning to predict the effects of cryoprotective agents on the GelMA-based bioinks used in extrusion cryobioprinting. Biodes Manuf 2023;6(4):464–77.
[105] Gui XY, Peng ZY, Song P, Chen L, Xu XJ, Li HR, et al. 3D printing of personalized polylactic acid scaffold laden with GelMA/autologous auricle cartilage to promote ear reconstruction. Biodes Manuf 2023;6(4):451–63.
[106] Sun HY, Ma HY, Wang L, Liu Y, Hou T, Tang WJ, et al. Biomimetic microchannel network with functional endothelium formed by sacrificial electrospun fibers inside 3D gelatin methacryloyl (GelMA) hydrogel models. J Zhejiang Univ Sci A 2024;25(1):79–96. Chinese.
[107] Van Hoorick J, Gruber P, Markovic M, Tromayer M, Van Erps J, Thienpont H, et al. Cross-linkable gelatins with superior mechanical properties through carboxylic acid modification: increasing the two-photon polymerization potential. Biomacromolecules 2017;18(10):3260–72.
[108] Rahimi F, Ahmadkhani N, Goodarzi A, Noori F, Hassanzadeh S, Saghati S, et al. Gelatin-based hydrogel functionalized with taurine moieties for *in vivo* skin tissue regeneration. Biodes Manuf 2023;6(3):284–97.
[109] Van den Bulcke AI, Bogdanov B, De Rooze N, Schacht EH, Cornelissen M, Berghmans H. Structural and rheological properties of methacrylamide modified gelatin hydrogels. Biomacromolecules 2000;1(1):31–8.
[110] Billiet T, Gasse BV, Gevaert E, Cornelissen M, Martins JC, Dubruel P. Quantitative contrasts in the photopolymerization of acrylamide and methacrylamide-functionalized gelatin hydrogel building blocks. Macromol Biosci 2013;13(11):1531–45.
[111] Van Hoorick J, Declercq H, De Muynck A, Houben A, Van Hoorebeke L, Cornelissen R, et al. Indirect additive manufacturing as an elegant tool for the production of self-supporting low density gelatin scaffolds. J Mater Sci Mater Med 2015;26(10):247.
[112] Zhao X, Lang Q, Yildirimer L, Lin ZY, Cui W, Annabi N, et al. Photocrosslinkable gelatin hydrogel for epidermal tissue engineering. Adv Healthc Mater 2016;5(1):108–18.
[113] Schuurman W, Levett PA, Pot MW, Van Weeren PR, Dhert WJA, Hutmacher DW, et al. Gelatin-methacrylamide hydrogels as potential biomaterials for fabrication of tissue-engineered cartilage constructs. Macromol Biosci 2013; 13(5):551–61.
[114] Ceylan H, Yasa IC, Yasa O, Tabak AF, Giltinan J, Sitti M. 3D-printed biodegradable microswimmer for theranostic cargo delivery and release. ACS Nano 2019;13(3):3353–62.
[115] Gao J, Liu X, Cheng J, Deng J, Han Z, Li M, et al. Application of photocrosslinkable hydrogels based on photolithography 3D bioprinting technology in bone tissue engineering. Regener Biomater 2023;10:rbad037.
[116] Kaehr B, Shear JB. Multiphoton fabrication of chemically responsive protein hydrogels for microactuation. Proc Natl Acad Sci USA 2008;105(26):8850–4.
[117] Chan BP, Ma JN, Xu JY, Li CW, Cheng JP, Cheng SH. Femto-second laser-based free writing of 3D protein microstructures and micropatterns with sub-micrometer features: a study on voxels, porosity, and cytocompatibility. Adv Funct Mater 2014;24(3):277–94.
[118] Kam D, Olender A, Rudich A, Kan-Tor Y, Buxboim A, Shoseyov O, et al. 3D printing of resilin in water by multiphoton absorption polymerization. Adv Funct Mater 2023;33(39):2210993.
[119] Kufelt O, El-Tamer A, Sehring C, Schlie-Wolter S, Chichkov BN. Hyaluronic acid based materials for scaffolding via two-photon polymerization. Biomacromolecules 2014;15(2):650–9.
[120] Qin XH, Gruber P, Markovic M, Plochberger B, Klotzsch E, Stampfl J, et al. Enzymatic synthesis of hyaluronic acid vinyl esters for two-photon microfabrication of biocompatible and biodegradable hydrogel constructs. Polym Chem 2014; 5(22):6523–33.
[121] Baudis S, Tomášiková Z, Zerobin E, Qin XH, Stampfl J, Ovsianikov A, et al. Additive manufactured, biocompatible hydrogels based on hyaluronic acid. In: Proceedings of the Conference Abstract: 10th World Biomaterials Congress; 2016 May 17–22; Montréal, Canada. Phoenix: Frontiers; 2016.
[122] Zerobin E, Markovic M, Tomášiková Z, Qin XH, Ret D, Steinbauer P, et al. Hyaluronic acid vinyl esters: a toolbox toward controlling mechanical properties of hydrogels for 3D microfabrication. J Polym Sci 2020;58(9):1288–98.
[123] Tao Y, Lu C, Deng C, Long J, Ren Y, Dai Z, et al. Four-dimensional stimuli-responsive hydrogels micro-structured via femtosecond laser additive manufacturing. Micromachines 2021;13(1):32.
[124] Duan Q, Zhang WC, Liu J, Jin F, Dong XZ, Bin FC, et al. 22 nm resolution achieved by femtosecond laser two-photon polymerization of a hyaluronic acid vinyl ester hydrogel. ACS Appl Mater Interfaces 2023;15(22):26472–83.
[125] Alcantar NA, Aydil ES, Israelachvili JN. Polyethylene glycol-coated biocompatible surfaces. J Biomed Mater Res 2000;51(3):343–51.
[126] Andrade JD, Hlady V, Jeon SI. Poly(ethylene oxide) and protein resistance. In: Hydrophilic polymers. Washington, DC: American Chemical Society; 1996. p. 51–9.
[127] Gölander CG, Herron JN, Lim K, Claesson P, Stenius P, Andrade JD. Properties of immobilized PEG films and the interaction with proteins. In: Harris JM, editor. Poly(ethylene glycol) chemistry: biotechnical and biomedical applications. Berlin: Springer; 1992. p. 221–45.
[128] Harris JM. Poly(ethylene glycol) chemistry: biotechnical and biomedical applications. Berlin: Springer Science & Business Media; 1992.
[129] Holmberg K, Bergström K, Stark MB. Immobilization of proteins via PEG chains. In: Harris JM, editor. Poly(ethylene glycol) chemistry: biotechnical and biomedical applications. Berlin: Springer; 1992. p. 303–24.
[130] Lee JH, Lee HB, Andrade JD. Blood compatibility of polyethylene oxide surfaces. Prog Polym Sci 1995;20(6):1043–79.
[131] Kirschner CM, Anseth KS. Hydrogels in healthcare: from static to dynamic material microenvironments. Diamond Jubilee Issue 2013;61(3):931–44.
[132] Place ES, George JH, Williams CK, Stevens MM. Synthetic polymer scaffolds for tissue engineering. Chem Soc Rev 2009;38(4):1139–51.
[133] Ivens IA, Achanzar W, Baumann A, Brändli-Baiocco A, Cavagnaro J, Dempster M, et al. PEGylated biopharmaceuticals: current experience and considerations for nonclinical development. Toxicol Pathol 2015;43(7):959–83.
[134] Turecek PL, Bossard MJ, Schoetens F, Ivens IA. PEGylation of biopharmaceuticals: a review of chemistry and nonclinical safety information of approved drugs. J Pharm Sci 2016;105(2):460–75.
[135] Dai Q, Walkey C, Chan WCW. Polyethylene glycol backfilling mitigates the negative impact of the protein corona on nanoparticle cell targeting. Angew Chem Int Ed 2014;53(20):5093–6.
[136] Liu M, Johansen P, Zabel F, Leroux JC, Gauthier MA. Semi-permeable coatings fabricated from comb-polymers efficiently protect proteins *in vivo*. Nat Commun 2014;5(1):5526.
[137] Manavitehrani I, Fathi A, Badr H, Daly S, Negahi Shirazi A, Dehghani F. Biomedical applications of biodegradable polyesters. Polymers 2016;8(1):20.
[138] Melissinaki V, Gill AA, Ortega I, Vamvakaki M, Ranella A, Haycock JW, et al. Direct laser writing of 3D scaffolds for neural tissue engineering applications. Biofabrication 2011;3(4):045005.
[139] Thompson JR, Worthington KS, Green BJ, Mullin NK, Jiao C, Kaalberg EE,

et al. Two-photon polymerized poly(caprolactone) retinal cell delivery scaffolds and their systemic and retinal biocompatibility. Acta Biomater 2019;94:204–18.
[140] Duffy DC, McDonald JC, Schueller OJA, Whitesides GM. Rapid prototyping of microfluidic systems in poly(dimethylsiloxane). Anal Chem 1998; 70(23): 4974–84.
[141] Ishikawa N, Hanada Y, Ishikawa I, Sugioka K, Midorikawa K. Femtosecond laser-fabricated biochip for studying symbiosis between *Phormidium* and seedling root. Appl Phys B 2015;119(3):503–8.
[142] Kant MB, Shinde SD, Bodas D, Patil KR, Sathe VG, Adhi KP, et al. Surface studies on benzophenone doped PDMS microstructures fabricated using KrF excimer laser direct write lithography. Appl Surf Sci 2014;314:292–300.
[143] Lee SJ, Goedert M, Matyska MT, Ghandehari EM, Vijay M, Pesek JJ. Polymethylhydrosiloxane (PMHS) as a functional material for microfluidic chips. J Micromech Microeng 2008;18(2):025026.
[144] Park JW, Vahidi B, Taylor AM, Rhee SW, Jeon NL. Microfluidic culture platform for neuroscience research. Nat Protoc 2006;1(4):2128–36.
[145] Takai M, Shirai T, Ishihara K. Surface functionarization of polydimethylsiloxane by photo-induced polymerization of 2-methacryloyloxyethyl phosphorylcholine for biodevices. J Photopolym Sci Technol 2011;24(5):597–602.
[146] Waheed S, Cabot JM, Macdonald NP, Lewis T, Guijt RM, Paull B, et al. 3D printed microfluidic devices: enablers and barriers. Lab Chip 2016;16(11):1993–2013.
[147] Coenjarts CA, Ober CK. Two-photon three-dimensional microfabrication of poly(dimethylsiloxane) elastomers. Chem Mater 2004;16(26):5556–8.
[148] Hasegawa T, Oishi K, Maruo S. Three-dimensional microstructuring of PDMS by two-photon microstereolithography. In: Proceedings of the 2006 IEEEInternational Symposium on MicroNanoMechanical and Human Science; 2006 Nov 5 – 8; Nagoya, Japan. Piscataway: IEEE; 2006. p. 1–4.
[149] Rekštytė S, Malinauskas M, Juodkazis S. Three-dimensional laser micro-sculpturing of silicone: towards bio-compatible scaffolds. Opt Express 2013; 21(14):17028–41.
[150] Gokaltun A, Yarmush ML, Asatekin A, Usta OB. Recent advances in nonbiofouling PDMS surface modification strategies applicable to microfluidic technology. Technology 2017;05(01):1–12.
[151] Tan SH, Nguyen NT, Chua YC, Kang TG. Oxygen plasma treatment for reducing hydrophobicity of a sealed polydimethylsiloxane microchannel. Biomicrofluidics 2010;4(3):032204.
[152] Wu MH, Urban JPG, Cui Z, Cui ZF. Development of PDMS microbioreactor with well-defined and homogenous culture environment for chondrocyte 3-D culture. Biomed Microdevices 2006;8(4):331–40.
[153] Nakano H, Kakinoki S, Iwasaki Y. Long-lasting hydrophilic surface generated on poly(dimethyl siloxane) with photoreactive zwitterionic polymers. Colloids Surf B Biointerfaces 2021;205:111900.
[154] Buchroithner B, Hartmann D, Mayr S, Oh YJ, Sivun D, Karner A, et al. 3D multiphoton lithography using biocompatible polymers with specific mechanical properties. Nanoscale Adv 2020;2(6):2422–8.
[155] Men L, Wang K, Hu N, Wang F, Deng Y, Zhang W, et al. Biocompatible polymers with tunable mechanical properties and conductive functionality on two-photon 3D printing. RSC Advances 2023;13(13):8586–93.
[156] del Pozo M, Sol JAHP, Schenning APHJ, Debije MG. 4D printing of liquid crystals: what's right for me? Adv Mater 2021;34(3):2104390.
[157] Xia Y, He Y, Zhang F, Liu Y, Leng J. A review of shape memory polymers and composites: mechanisms, materials, and applications. Adv Mater 2021; 33(6): 2000713.
[158] Xia H, Wang J, Tian Y, Chen QD, Du XB, Zhang YL, et al. Ferrofluids for fabrication of remotely controllable micro-nanomachines by two-photon polymerization. Adv Mater 2010;22(29):3204–7.
[159] Lee MR, Phang IY, Cui Y, Lee YH, Ling XY. Shape-shifting 3D protein microstructures with programmable directionality via quantitative nanoscale stiffness modulation. Small 2015;11(6):740–8.
[160] Sun YL, Dong WF, Yang RZ, Meng X, Zhang L, Chen QD, et al. Dynamically tunable protein microlenses. Angew Chem Int Ed 2012;51(7):1558–62.
[161] Ma ZC, Zhang YL, Han B, Hu XY, Li CH, Chen QD, et al. Femtosecond laser programmed artificial musculoskeletal systems. Nat Commun 2020;11(1):4536.
[162] Champeau M, Heinze DA, Viana TN, de Souza ER, Chinellato AC, Titotto S. 4D printing of hydrogels: a review. Adv Funct Mater 2020;30(31):1910606.
[163] Martella D, Antonioli D, Nocentini S, Wiersma DS, Galli G, Laus M, et al. Light activated non-reciprocal motion in liquid crystalline networks by designed microactuator architecture. RSC Advances 2017;7(32):19940–7.
[164] Zeng H, Wasylczyk P, Parmeggiani C, Martella D, Burresi M, Wiersma DS. Light-fueled microscopic walkers. Adv Mater 2015;27(26):3883–7.
[165] Martella D, Nocentini S, Nuzhdin D, Parmeggiani C, Wiersma DS. Photonic microhand with autonomous action. Adv Mater 2017;29(42):1704047.
[166] Elliott LV, Salzman EE, Greer JR. Stimuli responsive shape memory microarchitectures. Adv Funct Mater 2021;31(9):2008380.
[167] Peters C, Hoop M, Pané S, Nelson BJ, Hierold C. Degradable magnetic composites for minimally invasive interventions: device fabrication, targeted drug delivery, and cytotoxicity tests. Adv Mater 2016;28(3):533–8.
[168] Nguyen AK, Gittard SD, Koroleva A, Schlie S, Gaidukeviciute A, Chichkov BN, et al. Two-photon polymerization of polyethylene glycol diacrylate scaffolds with riboflavin and triethanolamine used as a water-soluble photoinitiator. Regen Med 2013;8(6):725–38.
[169] Do AV, Worthington KS, Tucker BA, Salem AK. Controlled drug delivery from 3D printed two-photon polymerized poly(ethylene glycol) dimethacrylate devices. Int J Pharm 2018;552(1–2):217–24.
[170] Kloxin AM, Kasko AM, Salinas CN, Anseth KS. Photodegradable hydrogels for dynamic tuning of physical and chemical properties. Science 2009;324(5923): 59–63.
[171] Arslan A, Steiger W, Roose P, Van den Bergen H, Gruber P, Zerobin E, et al. Polymer architecture as key to unprecedented high-resolution 3D-printing performance: the case of biodegradable hexa-functional telechelic urethane-based poly-e-caprolactone. Mater Today 2021;44:25–39.
[172] Felfel RM, Poocza L, Gimeno-Fabra M, Milde T, Hildebrand G, Ahmed I, et al. *In vitro* degradation and mechanical properties of PLA-PCL copolymer unit cell scaffolds generated by two-photon polymerization. Biomed Mater 2016; 11(1): 015011.
[173] Watanabe T, Akiyama M, Totani K, Kuebler SM, Stellacci F, Wenseleers W, et al. Photoresponsive hydrogel microstructure fabricated by two-photon initiated polymerization. Adv Funct Mater 2002;12(9):611–4.
[174] Hippler M, Blasco E, Qu J, Tanaka M, Barner-Kowollik C, Wegener M, et al. Controlling the shape of 3D microstructures by temperature and light. Nat Commun 2019;10(1):232.
[175] Lee YW, Kim JK, Bozuyuk U, Dogan NO, Khan MTA, Shiva A, et al. Multifunctional 3D-printed pollen grain-inspired hydrogel microrobots for on-demand anchoring and cargo delivery. Adv Mater 2023;35(10):2209812.
[176] Liese J, Hampp N. Synthesis and photocleavage of a new polymerizable [2+2] hetero dimer for phototriggered drug delivery. J Photochem Photobiol A 2011; 219(2–3):228–34.
[177] Neidinger P, Voll D, Walden SL, Unterreiner AN, Barner-Kowollik C. Two photon induced pulsed laser polymerization with near infrared light. ACS Macro Lett 2023;12(3):308–13.
[178] Jing X, Fu H, Yu B, Sun M, Wang L. Two-photon polymerization for 3D biomedical scaffolds: overview and updates. Front Bioeng Biotechnol 2022;10: 994355.
[179] Jia HY, Flommersfeld J, Heymann M, Vogel SK, Franquelim HG, Bruckner DB, et al. 3D printed protein-based robotic structures actuated by molecular motor assemblies. Nat Mater 2022;21(6):703–9.
[180] Cheng Z, Zhang N, Chang L, Qi P, Zhang L, Lin L, et al. Two-photon collagen crosslinking in *ex vivo* human corneal lenticules induced by near-infrared femtosecond laser. J Biophotonics 2023;16(2):e202200160.
[181] Basu S, Campagnola PJ. Properties of crosslinked protein matrices for tissue engineering applications synthesized by multiphoton excitation. J Biomed Mater Res A 2004;71A(2):359–68.
[182] Cui X, Soliman BG, Alcala-Orozco CR, Li J, Vis MAM, Santos M, et al. Rapid photocrosslinking of silk hydrogels with high cell density and enhanced shape fidelity. Adv Healthc Mater 2020;9(4):1901667.
[183] Soto F, Chrostowski R. Frontiers of medical micro/nanorobotics: *in vivo* applications and commercialization perspectives toward clinical uses. Front Bioeng Biotechnol 2018;6:170.
[184] Abbott JJ, Peyer KE, Lagomarsino MC, Zhang L, Dong L, Kaliakatsos IK, et al. How should microrobots swim? Int J Robot Res 2009;28(11–12):1434–47.
[185] Ghosh A, Fischer P. Controlled propulsion of artificial magnetic nanostructured propellers. Nano Lett 2009;9(6):2243–5.
[186] Peyer KE, Zhang L, Nelson BJ. Bio-inspired magnetic swimming microrobots for biomedical applications. Nanoscale 2013;5(4):1259–72.
[187] Li J, Li X, Luo T, Wang R, Liu C, Chen S, et al. Development of a magnetic microrobot for carrying and delivering targeted cells. Sci Robot 2018; 3(19): eaat8829.
[188] Nelson BJ, Pané S. Delivering drugs with microrobots. Science 2023;382(6675): 1120–2.
[189] Rapp T, DeForest C. Targeting drug delivery with light: a highly focused approach. Adv Drug Deliv Rev 2021;171:94–107.
[190] Yoshida K, Onoe H. Soft spiral-shaped microswimmers for autonomous swimming control by detecting surrounding environments. Adv Intell Syst 2020; 2(9):2000095.

[191] Li D, Liu Y, Yang Y, Shen Y. A fast and powerful swimming microrobot with a serrated tail enhanced propulsion interface. Nanoscale 2018;10(42):19673–7.
[192] Park J, Kim J, Pané S, Nelson BJ, Choi H. Acoustically mediated controlled drug release and targeted therapy with degradable 3D porous magnetic microrobots. Adv Healthc Mater 2021;10(2):2001096.
[193] Ren A, Hu JR, Qin CW, Xia N, Yu MF, Xu XB, et al. Oral administration microrobots for drug delivery. Bioact Mater 2024;39:163–90.
[194] Xin C, Yang L, Li J, Hu Y, Qian D, Fan S, et al. Conical hollow microhelices with superior swimming capabilities for targeted cargo delivery. Adv Mater 2019;31(25):1808226.
[195] Xu H, Medina-Sánchez M, Magdanz V, Schwarz L, Hebenstreit F, Schmidt OG. Sperm-hybrid micromotor for targeted drug delivery. ACS Nano 2018;12(1):327–37.
[196] Song X, Sun R, Wang R, Zhou K, Xie R, Lin J, et al. Puffball-inspired microrobotic systems with robust payload, strong protection, and targeted locomotion for on-demand drug delivery. Adv Mater 2022;34(43):2204791.
[197] Li Y, Dong D, Qu Y, Li J, Chen S, Zhao H, et al. A multidrug delivery microrobot for the synergistic treatment of cancer. Small 2023;19(44):2301889.
[198] Liu M, Du H, Zhang W, Zhai G. Internal stimuli-responsive nanocarriers for drug delivery: design strategies and applications. Mater Sci Eng C 2017; 71: 1267–80.
[199] Ye M, Zhou Y, Zhao H, Wang X. Magnetic microrobots with folate targeting for drug delivery. Cyborg Bionic Systems 2023;4:0019.
[200] Xin C, Jin DD, Hu YL, Yang L, Li R, Wang L, et al. Environmentally adaptive shape-morphing microrobots for localized cancer cell treatment. ACS Nano 2021;15(11):18048–59.
[201] Xin C, Jin D, Li R, Wang D, Ren Z, Liu B, et al. Rapid and multimaterial 4D printing of shape-morphing micromachines for narrow micronetworks traversing. Small 2022;18(37):2202272.
[202] Wang X, Chen XZ, Alcântara CCJ, Sevim S, Hoop M, Terzopoulou A, et al. MOFBOTS: metal–organic-framework-based biomedical microrobots. Adv Mater 2019;31(27):1901592.
[203] Hu Y, Wang Z, Jin D, Zhang C, Sun R, Li Z, et al. Botanical-inspired 4D printing of hydrogel at the microscale. Adv Funct Mater 2020;30(4):1907377.
[204] Wei S, Liu J, Zhao Y, Zhang T, Zheng M, Jin F, et al. Protein-based 3D microstructures with controllable morphology and pH-responsive properties. ACS Appl Mater Interfaces 2017;9(48):42247–57.
[205] Li R, Jin D, Pan D, Ji S, Xin C, Liu G, et al. Stimuli-responsive actuator fabricated by dynamic asymmetric femtosecond bessel beam for *in situ* particle and cell manipulation. ACS Nano 2020;14(5):5233–42.
[206] Zhou Y, Ye M, Zhao H, Wang X. 3D-printed PNAGA thermosensitive hydrogelbased microrobots: an effective cancer therapy by temperature-triggered drug release. Int J Bioprint 2023;9(3):709.
[207] Fujigaya T, Morimoto T, Nakashima N. Isolated single-walled carbon nanotubes in a gel as a molecular reservoir and its application to controlled drug release triggered by near-IR laser irradiation. Soft Matter 2011;7(6):2647–52.
[208] Deng CS, Liu YC, Fan XH, Jiao BZ, Zhang ZX, Zhang MD, et al. Femtosecond laser 4D printing of light-driven intelligent micromachines. Adv Funct Mater 2023;33(11):2211473.
[209] Bozuyuk U, Yasa O, Yasa IC, Ceylan H, Kizilel S, Sitti M. Light-triggered drug release from 3D-printed magnetic chitosan microswimmers. ACS Nano 2018; 12(9):9617–25.
[210] Yu M, Arteaga DN, Aksit A, Chiang H, Olson ES, Kysar JW, et al. Anatomical and functional consequences of microneedle perforation of round window membrane. Otol Neurotol 2020;41(2):e280–7.
[211] Wang Y, Sheng A, Jiang X, Yang S, Lin L, Yang M, et al. Multidrug dissolvable microneedle patch for the treatment of recurrent oral ulcer. Biodes Manuf 2023; 6(3):255–67.
[212] Aksit A, Arteaga DN, Arriaga M, Wang X, Watanabe H, Kasza KE, et al. *In-vitro* perforation of the round window membrane via direct 3-D printed microneedles. Biomed Microdevices 2018;20(2):47.
[213] Chiang H, Yu M, Aksit A, Wang W, Stern-Shavit S, Kysar JW, et al. 3D-printed microneedles create precise perforations in human round window membrane *in situ*. Otol Neurotol 2020;41(2):277–84.
[214] Aksit A, Rastogi S, Nadal ML, Parker AM, Lalwani AK, West AC, et al. Drug delivery device for the inner ear: ultra-sharp fully metallic microneedles. Drug Deliv Transl Res 2021;11(1):214–26.
[215] Balmert SC, Carey CD, Falo GD, Sethi SK, Erdos G, Korkmaz E, et al. Dissolving undercut microneedle arrays for multicomponent cutaneous vaccination. J Control Release 2020;317:336–46.
[216] Ebrahiminejad V, Faraji Rad Z, Prewett PD, Davies GJ. Fabrication and testing of polymer microneedles for transdermal drug delivery. Beilstein J Nanotechnol 2022;13:629–40.
[217] Faraji Rad Z, Nordon RE, Anthony CJ, Bilston L, Prewett PD, Arns JY, et al. High-fidelity replication of thermoplastic microneedles with open microfluidic channels. Microsyst Nanoeng 2017;3(1):17034.
[218] Faraji Rad Z, Prewett PD. Davies GJ Parametric optimization of two-photon direct laser writing process for manufacturing polymeric microneedles. Addit Manuf 2022;56:102953.
[219] Golpanian S, Schulman IH, Ebert RF, Heldman AW, DiFede DL, Yang PC, et al. Concise review: review and perspective of cell dosage and routes of administration from preclinical and clinical studies of stem cell therapy for heart disease. Stem Cells Transl Med 2016;5(2):186–91.
[220] Zakrzewski W, Dobrzyń ski M, Szymonowicz M, Rybak Z. Stem cells: past, present, and future. Stem Cell Res Ther 2019;10(1):68.
[221] Choi J, Hwang J, Kim J, Choi H. Recent progress in magnetically actuated microrobots for targeted delivery of therapeutic agents. Adv Healthc Mater 2021;10(6):2001596.
[222] Jeon S, Kim S, Ha S, Lee S, Kim E, Kim S, et al. Magnetically actuated microrobots as a platform for stem cell transplantation. Sci Robot 2019; 4(30): eaav4317.
[223] Dong M, Wang X, Chen XZ, Mushtaq F, Deng S, Zhu C, et al. 3D-printed soft magnetoelectric microswimmers for delivery and differentiation of neuron-like cells. Adv Funct Mater 2020;30(17):1910323.
[224] Wei T, Liu J, Li D, Chen S, Zhang Y, Li J, et al. Development of magnet-driven and image-guided degradable microrobots for the precise delivery of engineered stem cells for cancer therapy. Small 2020;16(41):1906908.
[225] Zhang C, Qiu X, Dai Y, Kong W, Liu Y, Niu H, et al. The prospects for bioprinting tumor models: recent advances in their applications. Biodes Manuf 2023;6(6):661–75.
[226] Du X, Chen Z, Li Q, Yang S, Jiang L, Yang Y, et al. Organoids revealed: morphological analysis of the profound next generation *in-vitro* model with artificial intelligence. Biodes Manuf 2023;6(3):319–39.
[227] Mazzocchi A, Soker S, Skardal A. 3D bioprinting for high-throughput screening: drug screening, disease modeling, and precision medicine applications. Appl Phys Rev 2019;6(1):011302.
[228] Low LA, Mummery C, Berridge BR, Austin CP, Tagle DA. Organs-on-chips: into the next decade. Nat Rev Drug Discov 2021;20(5):345–61.
[229] Liu Q, Mille LS, Villalobos C, Anaya I, Vostatek M, Yi S, et al. 3D-bioprinted cholangiocarcinoma-on-a-chip model for evaluating drug responses. Biodes Manuf 2023;6(4):373–89.
[230] Marino A, Tricinci O, Battaglini M, Filippeschi C, Mattoli V, Sinibaldi E, et al. A 3D real-scale, biomimetic, and biohybrid model of the blood-brain barrier fabricated through two-photon lithography. Small 2018;14(6):1702959.
[231] Tricinci O, De Pasquale D, Marino A, Battaglini M, Pucci C, Ciofani G. A 3D biohybrid real-scale model of the brain cancer microenvironment for advanced *in vitro* testing. Adv Mater Technol 2020;5(10):2000540.
[232] Marino A, Battaglini M, Carmignani A, Pignatelli F, De Pasquale D, Tricinci O, et al. Magnetic self-assembly of 3D multicellular microscaffolds: a biomimetic brain tumor-on-a-chip for drug delivery and selectivity testing. APL Bioeng 2023;7(3):036103.
[233] Michas C, Karakan MC, Nautiyal P, Seidman JG, Seidman CE, Agarwal A, et al. Engineering a living cardiac pump on a chip using high-precision fabrication. Sci Adv 2022;8(16):eabm3791.
[234] Zeußel L, Hampl J, Weise F, Singh S, Schober A. Bio-inspired 3D micro structuring of a liver lobule via direct laser writing: a comparative study with SU-8 and SUEX. J Laser Appl 2022;34(1):012007.
[235] Zhang L, Liu B, Wang C, Xin C, Li R, Wang D, et al. Functional shape-morphing microarchitectures fabricated by dynamic holographically shifted femtosecond multifoci. Nano Lett 2022;22(13):5277–86.
[236] Tayalia P, Mendonca CR, Baldacchini T, Mooney DJ, Mazur E. 3D cell-migration studies using two-photon engineered polymer scaffolds. Adv Mater 2008;20(23):4494–8.
[237] Barin N, Balcioglu HE, de Heer I, de Wit M, Lamfers MLM, van Royen ME, et al. 3D-engineered scaffolds to study microtubes and localization of epidermal growth factor receptor in patient-derived glioma cells. Small 2022; 18(49):2204485.
[238] Rengaraj A, Bosc L, Machillot P, McGuckin C, Milet C, Forraz N, et al. Engineering of a microscale niche for pancreatic tumor cells using bioactive film coatings combined with 3D-architectured scaffolds. ACS Appl Mater Interfaces 2022;14(11):13107–21.
[239] Langer R, Vacanti JP. Tissue engineering. Science 1993;260(5110):920–6.
[240] Moroni L, Burdick JA, Highley C, Lee SJ, Morimoto Y, Takeuchi S, et al. Biofabrication strategies for 3D *in vitro* models and regenerative medicine. Nat Rev Mater 2018;3(5):21–37.

[241] Groll J, Burdick JA, Cho DW, Derby B, Gelinsky M, Heilshorn SC, et al. A definition of bioinks and their distinction from biomaterial inks. Biofabrication 2018;11(1):013001.
[242] Fei PY, Ding HB, Duan Y, Wang XY, Hu W, Wu P, et al. Utility of TPP-manufactured biophysical restrictions to probe multiscale cellular dynamics. Biodes Manuf 2021;4(4):776–89.
[243] Tibbitt MW, Anseth KS. Dynamic microenvironments: the fourth dimension. Sci Transl Med 2012;4(160):160ps24.
[244] Akhmanova M, Osidak E, Domogatsky S, Rodin S, Domogatskaya A. Physical, spatial, and molecular aspects of extracellular matrix of *in vivo* niches and artificial scaffolds relevant to stem cells research. Stem Cells Int 2015; 2015: 167025.
[245] Greiner AM, Klein F, Gudzenko T, Richter B, Striebel T, Wundari BG, et al. Cell type-specific adaptation of cellular and nuclear volume in micro-engineered 3D environments. Biomaterials 2015;69:121–32.
[246] Klein F, Striebel T, Fischer J, Jiang Z, Franz CM, von Freymann G, et al. Elastic fully three-dimensional microstructure scaffolds for cell force measurements. Adv Mater 2010;22(8):868–71.
[247] Richter B, Hahn V, Bertels S, Claus TK, Wegener M, Delaittre G, et al. Guiding cell attachment in 3D microscaffolds selectively functionalized with two distinct adhesion proteins. Adv Mater 2017;29(5):1604342.
[248] Klein F, Richter B, Striebel T, Franz CM, von Freymann G, Wegener M, et al. Two-component polymer scaffolds for controlled three-dimensional cell culture. Adv Mater 2011;23(11):1341–5.
[249] Silva KR, Rezende RA, Pereira FDAS, Gruber P, Stuart MP, Ovsianikov A, et al. Delivery of human adipose stem cells spheroids into lockyballs. PLoS One 2016;11(11):e0166073.
[250] De Francesco F, Tirino V, Desiderio V, Ferraro G, D'Andrea F, Giuliano M, et al. Human $CD34^{+}$/$CD90^{+}$ ASCs are capable of growing as sphere clusters, producing high levels of VEGF and forming capillaries. PLoS One 2009;4(8): e6537.
[251] Ovsianikov A, Malinauskas M, Schlie S, Chichkov B, Gittard S, Narayan R, et al. Three-dimensional laser micro- and nano-structuring of acrylated poly (ethylene glycol) materials and evaluation of their cytoxicity for tissue engineering applications. Acta Biomater 2011;7(3):967–74.
[252] Mironov VA, Senatov FS, Koudan EV, Pereira FDAS, Kasyanov VA, Granjeiro JM, et al. Design, fabrication, and application of mini-scaffolds for cell components in tissue engineering. Polymers 2022;14(23):5068.
[253] Parkatzidis K, Chatzinikolaidou M, Kaliva M, Bakopoulou A, Farsari M, Vamvakaki M. Multiphoton 3D printing of biopolymer-based hydrogels. ACS Biomater Sci Eng 2019;5(11):6161–70.
[254] Claeyssens F, Hasan EA, Gaidukeviciute A, Achilleos DS, Ranella A, Reinhardt C, et al. Three-dimensional biodegradable structures fabricated by two-photon polymerization. Langmuir 2009;25(5):3219–23.
[255] Terzaki K, Kalloudi E, Mossou E, Mitchell EP, Forsyth VT, Rosseeva E, et al. Mineralized self-assembled peptides on 3D laser-made scaffolds: a new route toward 'scaffold on scaffold' hard tissue engineering. Biofabrication 2013;5(4): 045002.
[256] Koroleva A, Deiwick A, Nguyen A, Schlie-Wolter S, Narayan R, Timashev P, et al. Osteogenic differentiation of human mesenchymal stem cells in 3-D Zr-Si organic–inorganic scaffolds produced by two-photon polymerization technique. PLoS One 2015;10(2):e0118164.
[257] Timashev P, Kuznetsova D, Koroleva A, Prodanets N, Deiwick A, Piskun Y, et al. Novel biodegradable star-shaped polylactide scaffolds for bone regeneration fabricated by two-photon polymerization. Nanomedicine 2016;11(9):1041–53.
[258] Mihailescu M, Paun IA, Zamfirescu M, Luculescu CR, Acasandrei AM, Dinescu M. Laser-assisted fabrication and non-invasive imaging of 3D cell-seeding constructs for bone tissue engineering. J Mater Sci 2016;51(9):4262–73.
[259] Felfel RM, Gupta D, Zabidi AZ, Prosser A, Scotchford CA, Sottile V, et al. Performance of multiphase scaffolds for bone repair based on two-photon polymerized poly(*D*,*L*-lactide-*co*-ε-caprolactone), recombinamers hydrogel and nano-HA. Mater Des 2018;160:455–67.
[260] Weisgrab G, Guillaume O, Guo Z, Heimel P, Slezak P, Poot A, et al. 3D printing of large-scale and highly porous biodegradable tissue engineering scaffolds from poly(trimethylene-carbonate) using two-photon-polymerization. Biofabrication 2020;12(4):045036.
[261] Nouri-Goushki M, Isaakidou A, Eijkel BIM, Minneboo M, Liu Q, Boukany PE, et al. 3D printed submicron patterns orchestrate the response of macrophages. Nanoscale 2021;13(34):14304–15.
[262] Li J, Esteban-Fernández de Ávila B, Gao W, Zhang L, Wang J. Micro/nanorobots for biomedicine: delivery, surgery, sensing, and detoxification. Sci Robot 2017;2(4):eaam6431.
[263] DEJGJDolmans, Fukumura D, Jain RK. Photodynamic therapy for cancer. Nat Rev Cancer 2003;3(5):380–7.
[264] Moore CM, Pendse D, Emberton M. Photodynamic therapy for prostate cancer—a review of current status and future promise. Nat Clin Pract Urol 2009;6(1):18–30.
[265] Zhang Z, Huang W, Lei M, He Y, Yan M, Zhang X, et al. Laser-triggered intraocular implant to induce photodynamic therapy for posterior capsule opacification prevention. Int J Pharm 2016;498(1–2):1–11.
[266] Wang SW, Lei M. Recent advances in two-photon excited photodynamic therapy. Chin J Lasers 2022;49(15):1507101. Chinese.
[267] Sztandera K, Gorzkiewicz M, Klajnert-Maculewicz B. Nanocarriers in photodynamic therapy—*in vitro* and *in vivo* studies. Wires Nanomed Nanobi 2020;12(3):e1509.
[268] Starkey JR, Rebane AK, Drobizhev MA, Meng F, Gong A, Elliott A, et al. New two-photon activated photodynamic therapy sensitizers induce xenograft tumor regressions after near-IR laser treatment through the body of the host mouse. Clin Cancer Res 2008;14(20):6564–73.
[269] Guo L, Ge J, Liu Q, Jia Q, Zhang H, Liu W, et al. Versatile polymer nanoparticles as two-photon-triggered photosensitizers for simultaneous cellular, deep-tissue imaging, and photodynamic therapy. Adv Healthc Mater 2017; 6(12):1601431.
[270] Huang Y, Qiu F, Shen L, Chen D, Su Y, Yang C, et al. Combining two-photon-activated fluorescence resonance energy transfer and near-infrared photothermal effect of unimolecular micelles for enhanced photodynamic therapy. ACS Nano 2016;10(11):10489–99.
[271] Kim C, Gao R, Sei E, Brandt R, Hartman J, Hatschek T, et al. Chemoresistance evolution in triple-negative breast cancer delineated by single-cell sequencing. Cell 2018;173(4):879–93.
[272] Wagner DE, Weinreb C, Collins ZM, Briggs JA, Megason SG, Klein AM. Single-cell mapping of gene expression landscapes and lineage in the zebrafish embryo. Science 2018;360(6392):981–7.
[273] Zhou F, Li X, Wang W, Zhu P, Zhou J, He W, et al. Tracing haematopoietic stem cell formation at single-cell resolution. Nature 2016;533(7604):487–92.
[274] Alapan Y, Yigit B, Beker O, Demirörs AF, Sitti M. Shape-encoded dynamic assembly of mobile micromachines. Nat Mater 2019;18(11):1244–51.
[275] Hu XH, Yasa IC, Ren ZY, Goudu SR, Ceylan H, Hu WQ, et al. Magnetic soft micromachines made of linked microactuator networks. Sci Adv 2021; 7(23): eabe8436.
[276] Wang JY, Jin F, Dong XZ, Liu J, Zheng ML. Flytrap inspired pH-driven 3D hydrogel actuator by femtosecond laser microfabrication. Adv Mater Technol 2022;7(8):2200276.
[277] Yagoub SH, Thompson JG, Orth A, Dholakia K, Gibson BC, Dunning KR. Fabrication on the microscale: a two-photon polymerized device for oocyte microinjection. J Assist Reprod Genet 2022;39(7):1503–13.
[278] Nagrath S, Sequist LV, Maheswaran S, Bell DW, Irimia D, Ulkus L, et al. Isolation of rare circulating tumour cells in cancer patients by microchip technology. Nature 2007;450(7173):1235–9.
[279] Wyatt Shields CIV, Reyes CD, López GP. Microfluidic cell sorting: a review of the advances in the separation of cells from debulking to rare cell isolation. Lab Chip 2015;15(5):1230–49.
[280] Wang X, Papautsky I. Size-based microfluidic multimodal microparticle sorter. Lab Chip 2015;15(5):1350–9.
[281] Xu B, Hu W, Du W, Hu Y, Zhang C, Lao Z, et al. Arch-like microsorters with multi-modal and clogging-improved filtering functions by using femtosecond laser multifocal parallel microfabrication. Opt Express 2017;25(14):16739–53.
[282] Perrucci F, Bertana V, Marasso SL, Scordo G, Ferrero S, Pirri CF, et al. Optimization of a suspended two photon polymerized microfluidic filtration system. Microelectron Eng 2018;195:95–100.
[283] Zhang D, Men L, Chen Q. Femtosecond laser microfabricated microfilters for particle–liquid separation in a microfluidic chip. IEEE J Sel Top Quantum Electron 2019;25(1):1–7.
[284] Hu K, Yang L, Jin D, Li J, Ji S, Xin C, et al. Tunable microfluidic device fabricated by femtosecond structured light for particle and cell manipulation. Lab Chip 2019;19(23):3988–96.
[285] Kaynak M, Dirix P, Sakar MS. Addressable acoustic actuation of 3D printed soft robotic microsystems. Adv Sci 2020;7(20):2001120.
[286] Wang C, Hu Z, Yang L, Zhang C, Zhang L, Ji S, et al. Magnetically driven rotary microfilter fabricated by two-photon polymerization for multimode filtering of particles. Opt Lett 2021;46(12):2968–71.
[287] Xing Y, Zhao L, Cheng Z, Lv C, Yu F, Yu F. Microfluidics-based sensing of biospecies. ACS Appl Bio Mater 2021;4(3):2160–91.
[288] Yang SM, Lv S, Zhang W, Cui Y. Microfluidic Point-of-care (POC) devices in

early diagnosis: a review of opportunities and challenges. Sensors 2022;22(4):1620.
[289] Vora LK, Sabri AH, McKenna PE, Himawan A, Hutton ARJ, Detamornrat U, et al. Microneedle-based biosensing. Nat Rev Bioeng 2023;2:64–81.
[290] Friedel M, Thompson IAP, Kasting G, Polsky R, Cunningham D, Soh HT, et al. Opportunities and challenges in the diagnostic utility of dermal interstitial fluid. Nat Biomed Eng 2023;7(12):1541–55.
[291] AI-Abaddi M, Sasso L, Dimaki M, Svendsen W. Fabrication of 3D nano/microelectrodes via two-photon-polymerization. Microelectron Eng 2012; 98: 378–81.
[292] Haque MA, Lavrik NV, Hensley D, Briggs DP, McFarlane N. Carbonized polymer for joule heating processing towards biosensor development. In: Proceedings of the 2021 43rd Annual International Conference of the IEEE Engineering in Medicine & Biology Society (EMBC); 2021 Nov 1–5; Mexico. Piscataway: IEEE; 2021. p. 7578–81.
[293] Abu Shihada J, Jung M, Decke S, Koschinski L, Musall S, Rincón Montes V, et al. Highly customizable 3D microelectrode arrays for *in vitro* and *in vivo* neuronal tissue recordings. Adv Sci 2024;11(13):2305944.
[294] Miller PR, Xiao X, Brener I, Burckel DB, Narayan R, Polsky R. Microneedle-based transdermal sensor for on-chip potentiometric determination of K^+. Adv Healthc Mater 2014;3(6):876–81.
[295] Miller P, Moorman M, Manginell R, Ashlee C, Brener I, Wheeler D, et al. Towards an integrated microneedle total analysis chip for protein detection. Electroanalysis 2016;28(6):1305–10.
[296] Wollhofen R, Axmann M, Freudenthaler P, Gabriel C, Röhrl C, Stangl H, et al. Multiphoton-polymerized 3D protein assay. ACS Appl Mater Interfaces 2018; 10(2):1474–9.
[297] Trautmann A, Roth GL, Nujiqi B, Walther T, Hellmann R. Towards a versatile point-of-care system combining femtosecond laser generated microfluidic channels and direct laser written microneedle arrays. Microsyst Nanoeng 2019;5(1):6.
[298] Suzuki M, Takahashi T, Aoyagi S. 3D laser lithographic fabrication of hollow microneedle mimicking mosquitos and its characterisation. Int J Nanotechnol 2018;15(1–3):157–73.
[299] Li B, Tan H, Anastasova S, Power M, Seichepine F, Yang GZ. A bio-inspired 3D micro-structure for graphene-based bacteria sensing. Biosens Bioelectron 2019;123:77–84.
[300] Lao Z, Zheng Y, Dai Y, Hu Y, Ni J, Ji S, et al. Nanogap plasmonic structures fabricated by switchable capillary-force driven self-assembly for localized sensing of anticancer medicines with microfluidic SERS. Adv Funct Mater 2020;30(15):1909467.
[301] Chen S, Tan Z, Liao P, Li Y, Qu Y, Zhang Q, et al. Biodegradable microrobots for DNA vaccine delivery. Adv Healthc Mater 2023;12(21):2202921.
[302] Worthington KS, Wiley LA, Kaalberg EE, Collins MM, Mullins RF, Stone EM, et al. Two-photon polymerization for production of human iPSC-derived retinal cell grafts. Acta Biomater 2017;55:385–95.
[303] Lee YW, Ceylan H, Yasa IC, Kilic U, Sitti M. 3D-printed multi-stimuli-responsive mobile micromachines. ACS Appl Mater Interfaces 2021; 13(11): 12759–66.
[304] Yasa IC, Ceylan H, Bozuyuk U, Wild AM, Sitti M. Elucidating the interaction dynamics between microswimmer body and immune system for medical microrobots. Sci Robot 2020;5(43):eaaz3867.
[305] Geng Q, Wang D, Chen P, Chen SC. Ultrafast multi-focus 3-D nano-fabrication based on two-photon polymerization. Nat Commun 2019;10(1):2179.
[306] Saha S, Wang D, Nguyen V, Chang Y, Oakdale J, Chen S. Scalable submicrometer additive manufacturing. Science 2019;366(6461):105–9.
[307] Ouyang W, Xu X, Lu W, Zhao N, Han F, Chen SC. Ultrafast 3D nanofabrication via digital holography. Nat Commun 2023;14(1):1716.
[308] Lee XY, Saha SK, Sarkar S, Giera B. Automated detection of part quality during two-photon lithography via deep learning. Addit Manuf 2020;36:101444.
[309] Pingali R, Saha SK. Printability prediction in projection two-photon lithography via machine learning based surrogate modeling of photopolymerization. J Micro Nano Sci Eng 2022;10(3):031005.
[310] Jia S, Sun J, Howes A, Dawson MR, Toussaint Jr KC, Shao C. Hybrid physics-guided data-driven modeling for generalizable geometric accuracy prediction and improvement in two-photon lithography. J Manuf Process 2024;110:202–10.
[311] Wang S, Yu Y, Liu H, Lim KTP, Srinivasan BM, Zhang YW, et al. Sub-10-nm suspended nano-web formation by direct laser writing. Nano Futures 2018;2(2): 025006.
[312] Tan L, Lee H, Fang L, Cappelleri DJJ. A power compensation strategy for achieving homogeneous microstructures for 4D printing shape-adaptive PNIPAM hydrogels: out-of-plane variations. Gels 2022;8(12):828.
[313] Aderneuer T, Fernández O, Ferrini R. Two-photon grayscale lithography for free-form micro-optical arrays. Opt Express 2021;29(24):39511.
[314] Lamprecht B, Ulm A, Lichtenegger P, Leiner C, Nemitz W, Sommer C. Origination of free-form micro-optical elements using one- and two-photon grayscale laser lithography. Appl Opt 2022;61(8):1863.
[315] Rodríguez S. Redefining microfabrication of high-precision optics. Photonics Views 2020;17(1):36–9.
[316] Mayer F, Richter S, Westhauser J, Blasco E, Barner-Kowollik C, Wegener M. Multimaterial 3D laser microprinting using an integrated microfluidic system. Sci Adv 2019;5(2):eaau9160.
[317] Sanders SN, Schloemer TH, Gangishetty MK, Anderson D, Seitz M, Gallegos AO, et al. Triplet fusion upconversion nanocapsules for volumetric 3D printing. Nature 2022;604(7906):474–8.
[318] Hahn V, Messer T, Bojanowski NM, Curticean ER, Wacker I, Schröder RR, et al. Two-step absorption instead of two-photon absorption in 3D nanoprinting. Nat Photonics 2021;15(12):932–8.
[319] Hahn V, Rietz P, Hermann F, Müller P, Barner-Kowollik C, Schlöder T, et al. Light-sheet 3D microprinting via two-colour two-step absorption. Nat Photonics 2022;16(11):784–91.